Quantum Hall Effect without Applied Magnetic Field

Guang-Yu Guo (郭光宇)

Physics Department, National Taiwan University, Taiwan

(Colloquium Talk in NTU Physics Dept., Oct. 4, 2016)

Plan of this Talk

I. Introduction

1. (Integer) quantum Hall effect
2. Spontaneous quantum Hall effects (SQHE)
3. Why search for SQHE in layered 4d and 5d transition metal oxides

II. Chern insulator in 4d and 5d transition metal perovskite bilayers

1. 4d and 5d metal perovskite bilayers along [111] direction
2. Magnetic and electronic properties
3. Quantum anomalous Hall phase

III. Quantum topological Hall effect in chiral antiferromagnet $K_{1/2}RhO_2$

1. Physical properties of layered oxide K_xRhO_2
2. Non-coplanar antiferromagnetic ground state structure
3. Unconventional quantum anomalous Hall phase

IV. Conclusions

I. Introduction

1. (Integer) quantum Hall effect

1) Ordinal Hall Effect [Hall 1879]

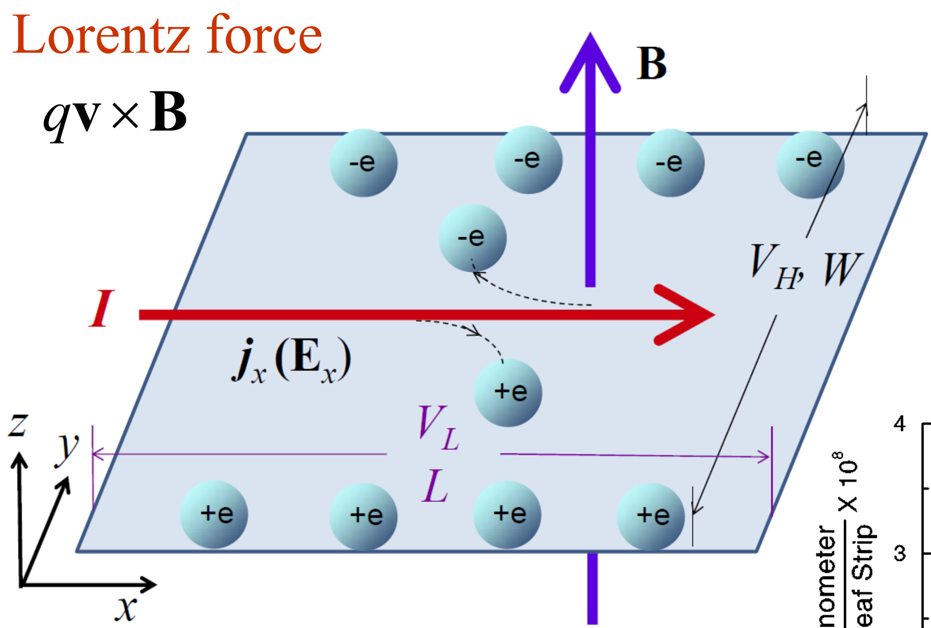

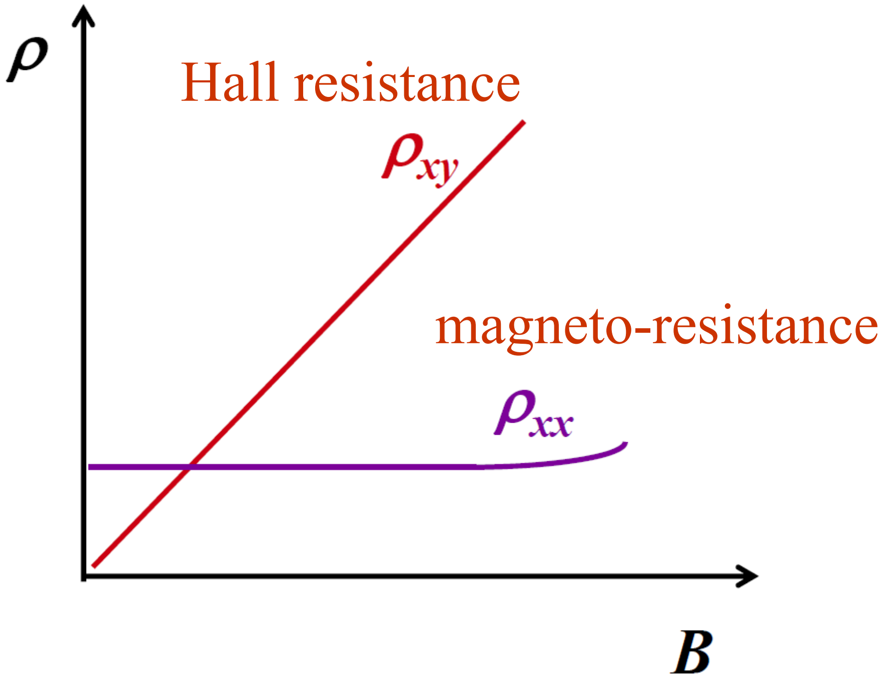

$$R_L = V_L / I = (E_x L)/(j_x W)$$
$$= \rho_{xx}(L/W)$$

$$R_H = V_H / I = (E_y W)/(j_x W) = \rho_{xy}$$
$$= (1/nq)B$$

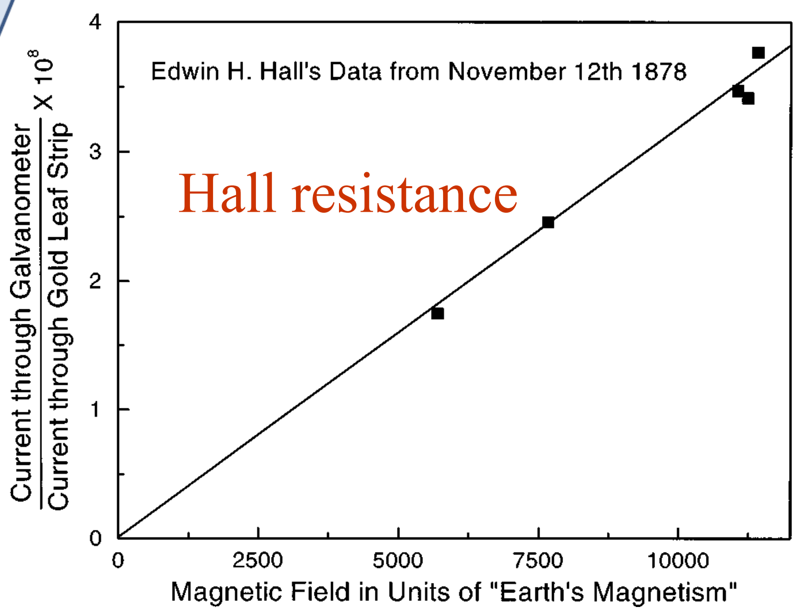

Edwin H. Hall (1855-1938)

OHE is a widely used characterization tool in material science lab.

2) (Integer) quantum Hall Effect [von Klitzing et al., 1980]

In 1980, von Klitzing et al discovered QHE. [PRL 45, 494]

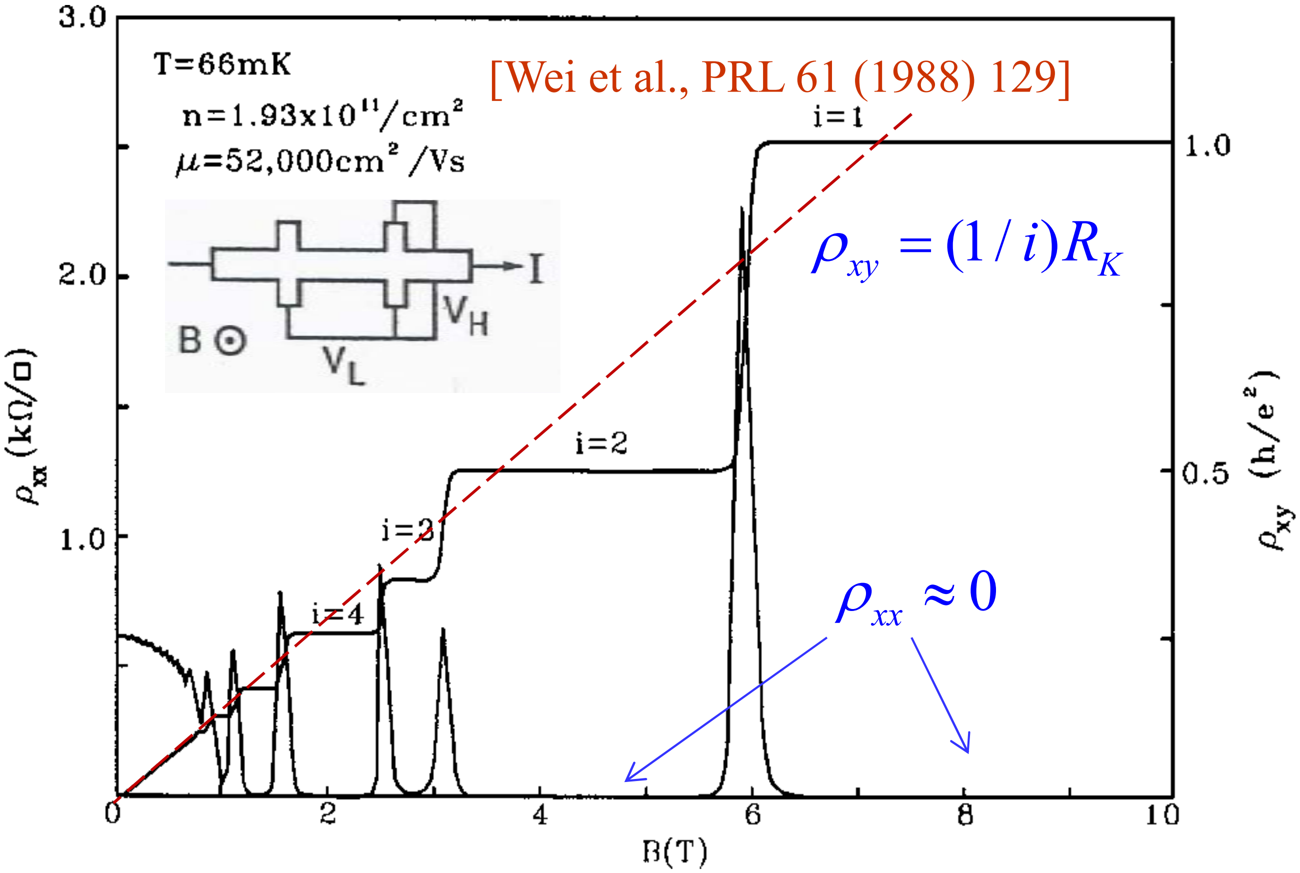

Klaus von Klitzing (1943-present)

von Klitzing constant

$R_K = 1\ \mathrm{h/e^2}$

$= 25812.807557(18)\ \Omega$

Conductance quantum

$\sigma_0 = 1/R_K = 1\ \mathrm{e^2/h}$

$\rho_{xx} \approx 0$, superconducting states ($\sigma_{xx} \approx \infty$)?

$$\boldsymbol{\rho} = \begin{pmatrix} 0 & \rho_{xy} \\ -\rho_{xy} & 0 \end{pmatrix}, \ \boldsymbol{\sigma} = [\boldsymbol{\rho}]^{-1} = \begin{pmatrix} 0 & -1/\rho_{xy} \\ 1/\rho_{xy} & 0 \end{pmatrix},$$

$\sigma_{xy} = -1/\rho_{xy} = i\sigma_0,\ \sigma_{xx} = 0,$ they are insulating phases.

Formation of discrete Landau levels

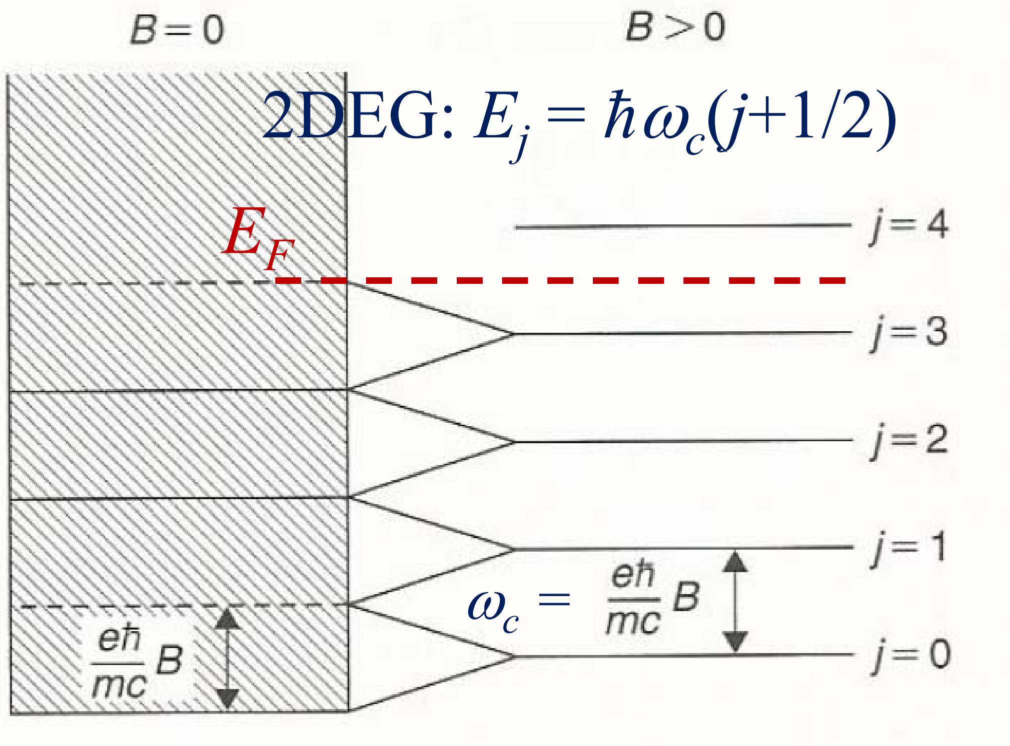

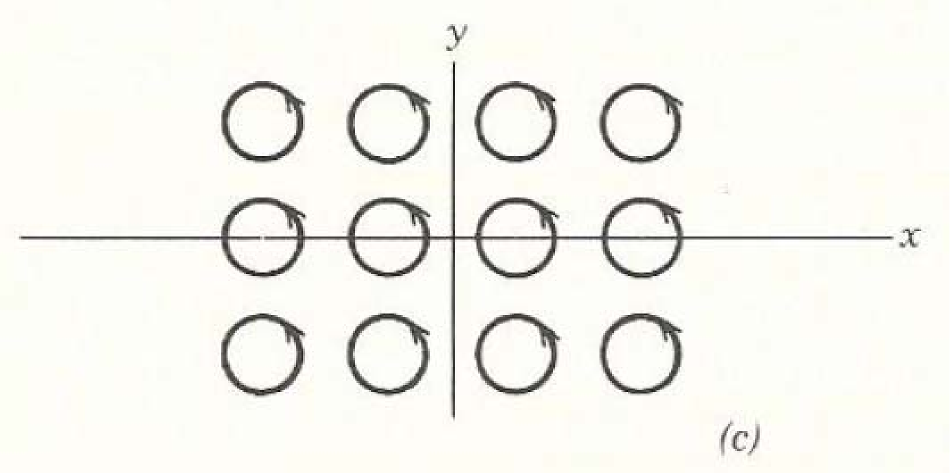

Bulk quantum Hall insulating state

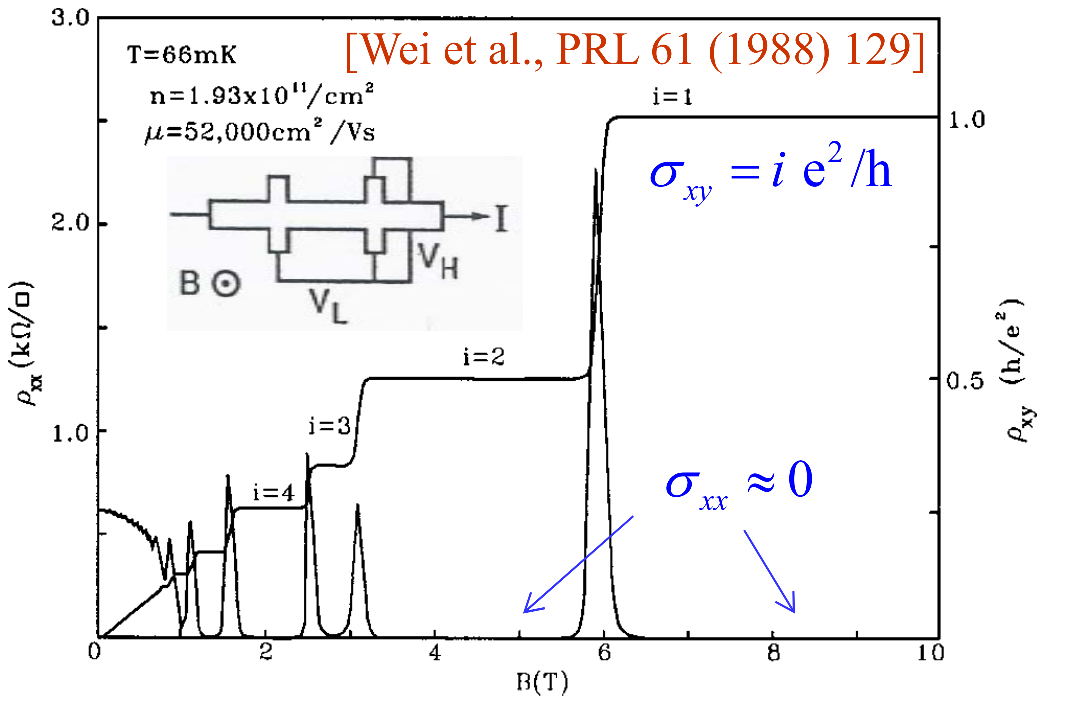

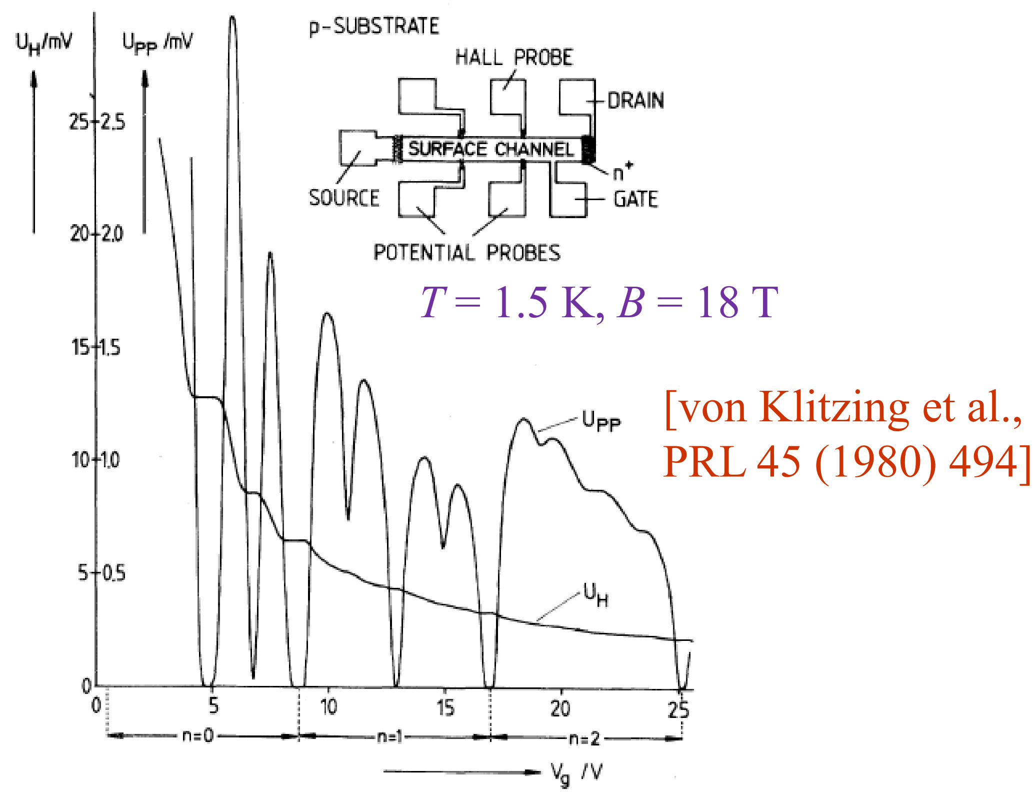

Quantization of Hall conductance

Thouless et al. topological invariance argument

[PRL49, 405 (1982); PRB31, 3372 (1985)]

$$\sigma_{xy} = n\frac{2e^2}{h}, \; n = \text{Chern (TKNN) number}$$

(Berry curvature)

$$n = \frac{1}{2\pi}\sum_i \int_{\substack{\text{2D}\\ \text{BZ}}} dk_x dk_x \Omega_z^i(\mathbf{k}), \; \Omega_z^i(\mathbf{k}) = i\left(\left\langle \frac{\partial u_{i\mathbf{k}}}{\partial k_x}\middle|\frac{\partial u_{i\mathbf{k}}}{\partial k_y}\right\rangle - \left\langle \frac{\partial u_{i\mathbf{k}}}{\partial k_y}\middle|\frac{\partial u_{i\mathbf{k}}}{\partial k_x}\right\rangle\right)$$

David Thouless (1934 -)

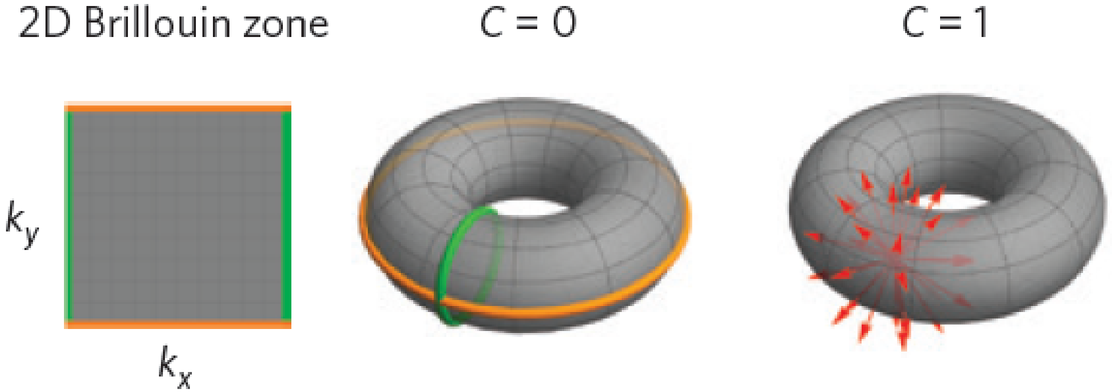

2D BZ is a torus. Chern theorem:

$$\int_{\substack{\text{2D}\\ \text{BZ}}} dk_x dk_x \Omega_z(\mathbf{k}) = \int_S \Omega(\mathbf{k})\cdot dS = 2\pi C.$$

QH phases are the first discovered topological phases of quantum matter; QH systems are the first topological insulators with broken time-reversal symmetry. Topological invariant is Chern number.

Q: A nonzero conductance in an insulating system! How can it be possible?

Existence of conducting edge states (modes)

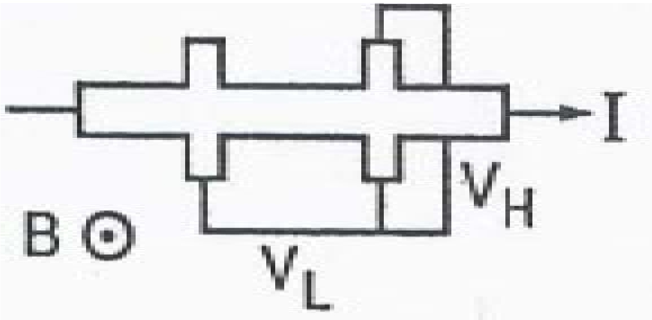

To do measurements, a finite size sample and hence boundaries must be created.

(a) Laughlin gauge invariance argument

[Laughlin, PRB23 (1981) 5632; Halperin, PRB25 (1982) 4802]

Robert Laughlin (1950 -)

(b) Bulk-edge correspondence theorem

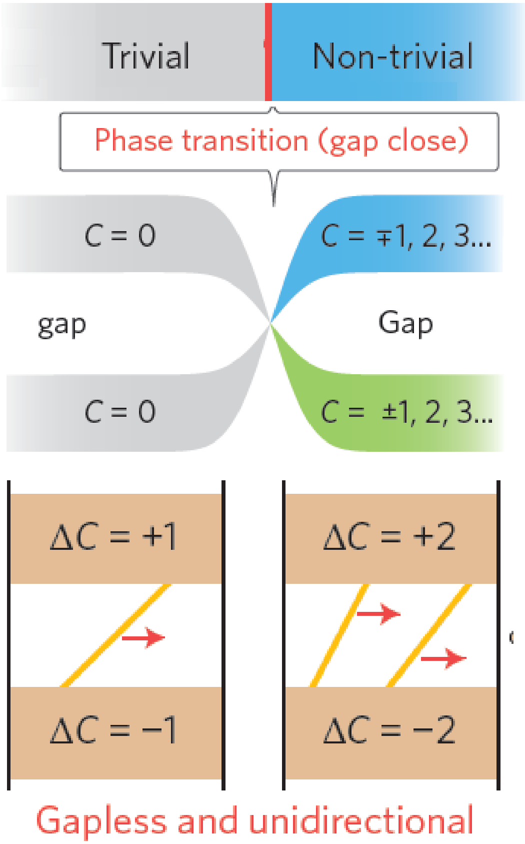

When crossing the boundary between two different Chern insulators, the band gap would close and open again, i.e., metallic edge states exist at the edge whose number is equal to the difference in Chern number.

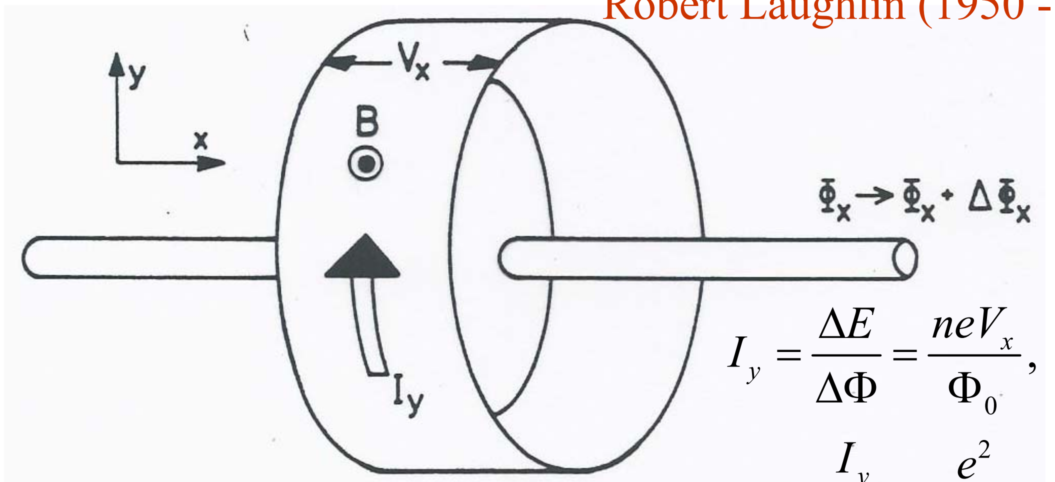

$$I_y = \frac{\Delta E}{\Delta \Phi} = \frac{neV_x}{\Phi_0},$$

$$\sigma_{xy} = \frac{I_y}{V_x} = n\frac{e^2}{h}.$$

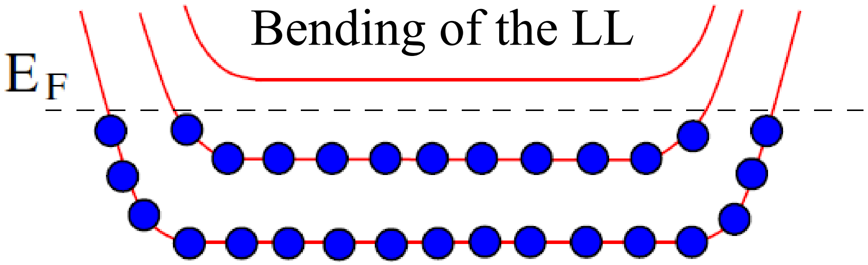

(c) Explicit energy band calculations

[Hatsugai, PRL 71 (1993) 3697]

IQHE is an intriguing phenomenon due to the occurrence of bulk topological insulating phases with dissipationless conducting edge states in the Hall bars at low temperatures and under strong magnetic field. Hall resistance is so precisely quantized that it can be used to determine the fundamental constants and robust metallic edge state is useful for low-power consuming nanoelectronics and spintronics.

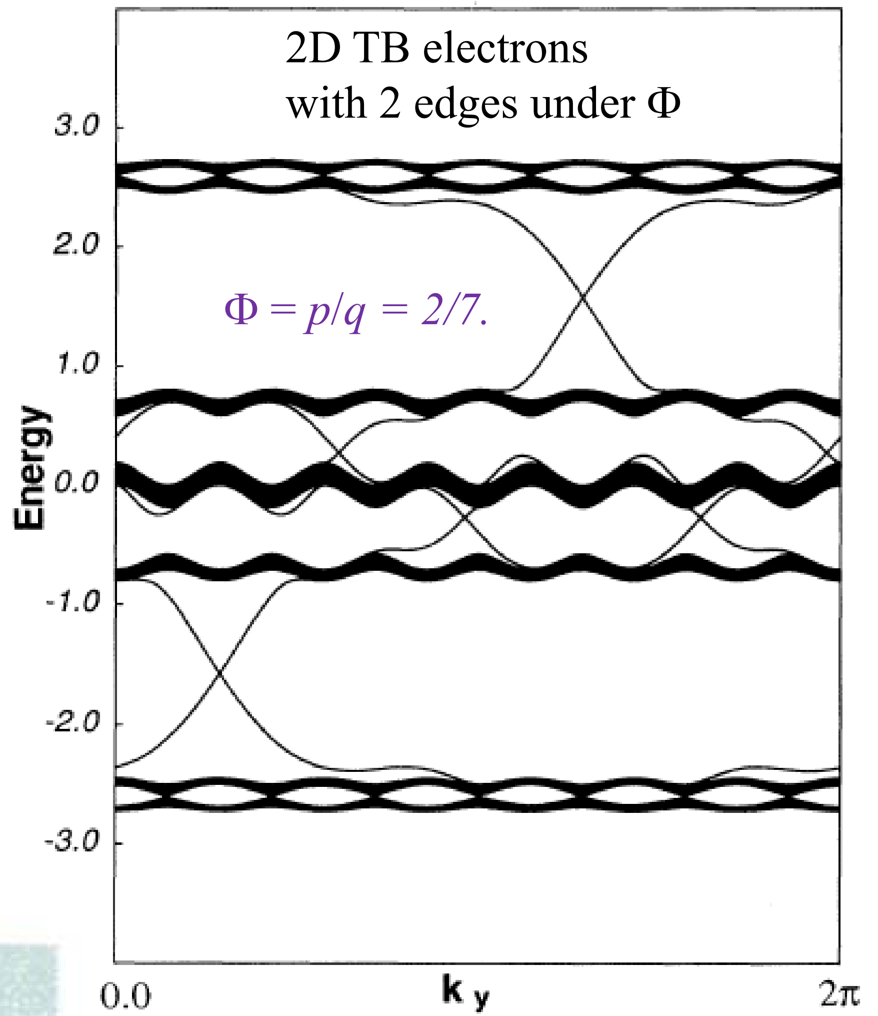

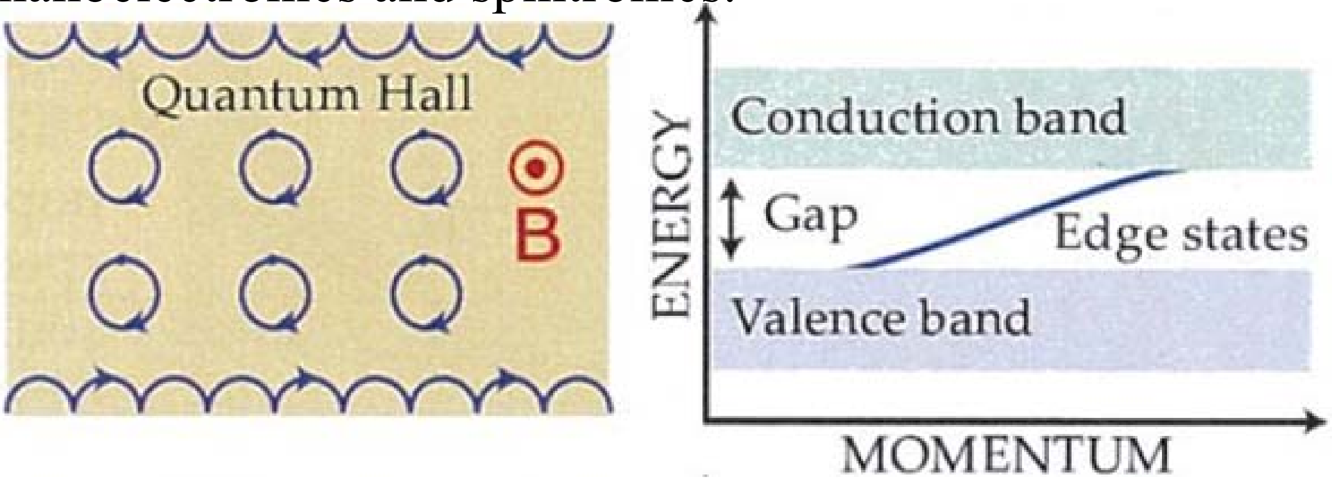

Q: High temperature IQHE without applied magnetic field?

2. Spontaneous quantum Hall effects

1) Anomalous Hall Effect [Hall 1881]

(Hall effect with applied magnetic field)

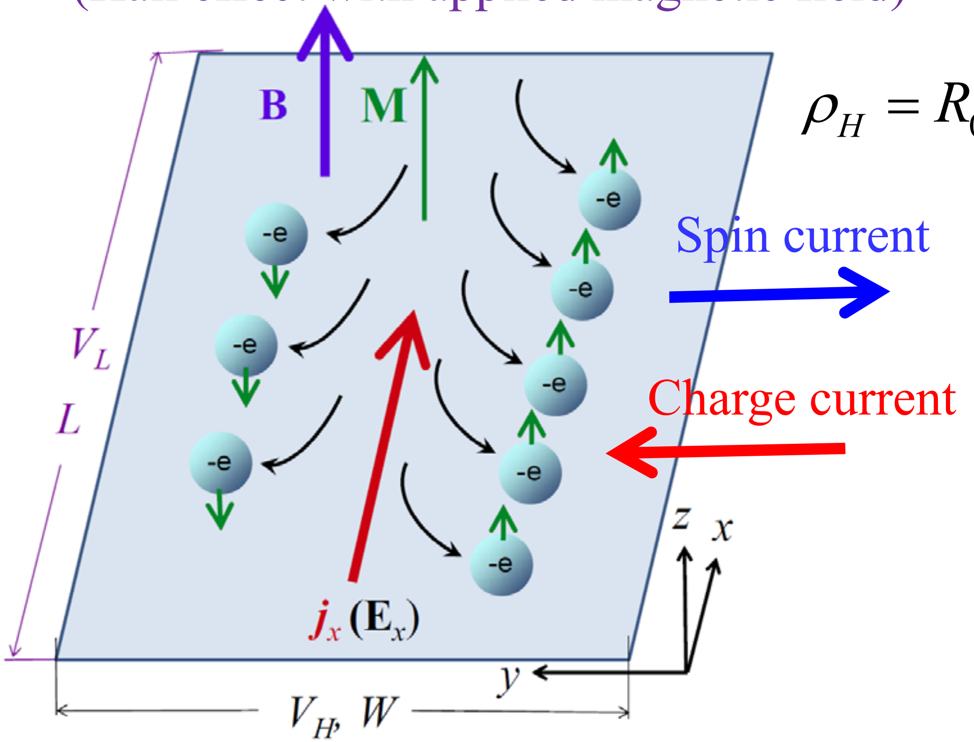

$$\rho_H = R_0 B + R_S M$$

Mn_5Ge_3 [Zeng et al. PRL 96 (2006) 2010]

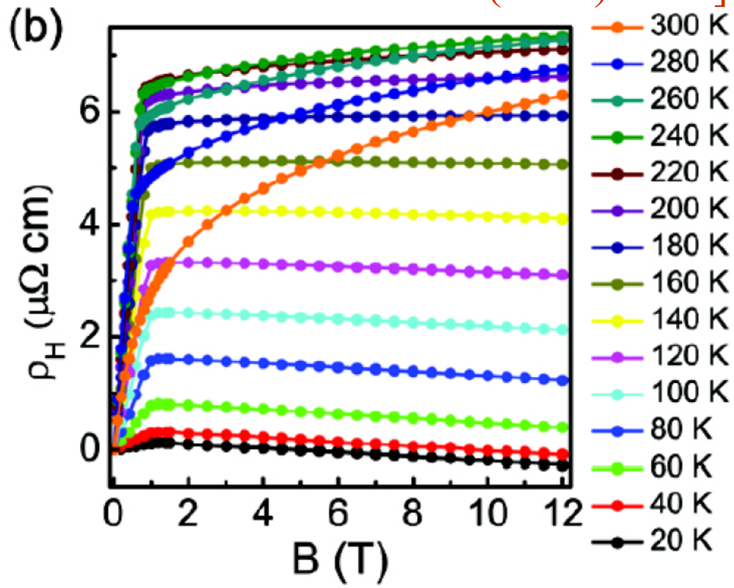

Relativistic spin-orbit coupling [Jackson's textbook]

$$\vec{B}' = -\gamma \frac{\vec{v}}{c} \times \vec{E} \simeq \left(\frac{\vec{E}\times\vec{p}}{mc}\right),$$

$$H_{SO} = -\vec{\mu}\cdot\vec{B}' = -\frac{1}{2m^2c^2}\vec{s}\cdot(\nabla V(\mathbf{r})\times\vec{p})$$

$$H_{SO} = -\frac{1}{2m^2c^2}\vec{s}\cdot\left(\frac{dV}{dr}\frac{\vec{r}}{r}\times\vec{p}\right) \approx -\frac{Ze^2}{2m^2c^2r^3}(\vec{s}\cdot\vec{L})$$

(Mott or skew scattering)

2) Spin Hall Effect

[Dyakonov & Perel, JETP 1971]

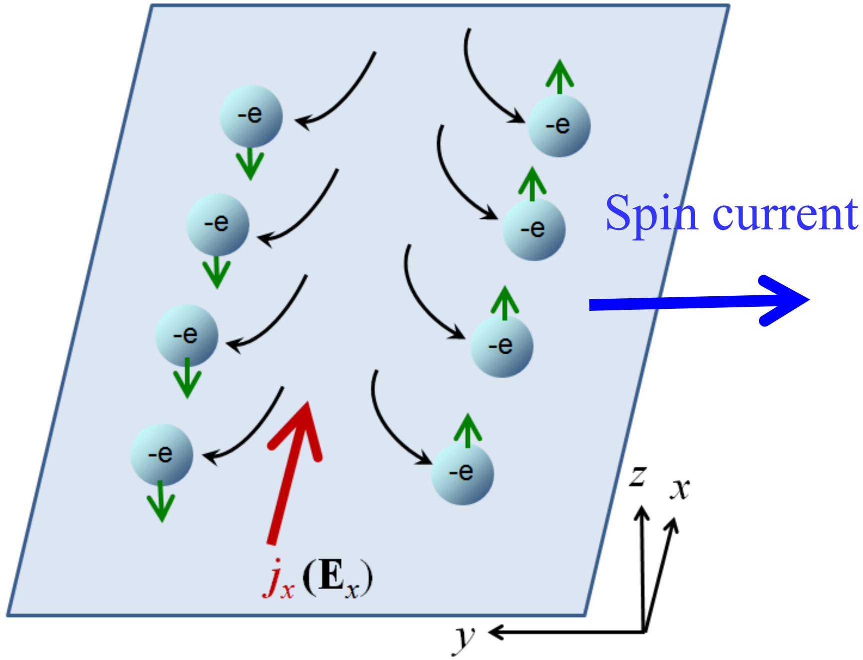

3) Quantum spin Hall effect and topological insulators

(a) Intrinsic spin Hall effect

[Science 301, 1348 (2003)]

Dissipationless Quantum Spin Current at Room Temperature

Shuichi Murakami,[1*] Naoto Nagaosa,[1,2,3] Shou-Cheng Zhang[4]

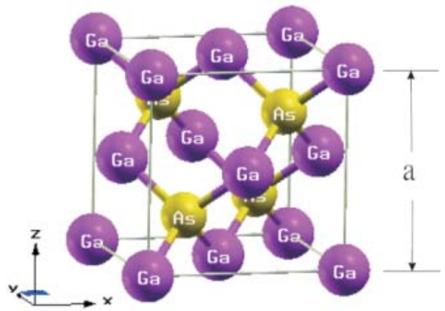

p-type zincblende semiconductors

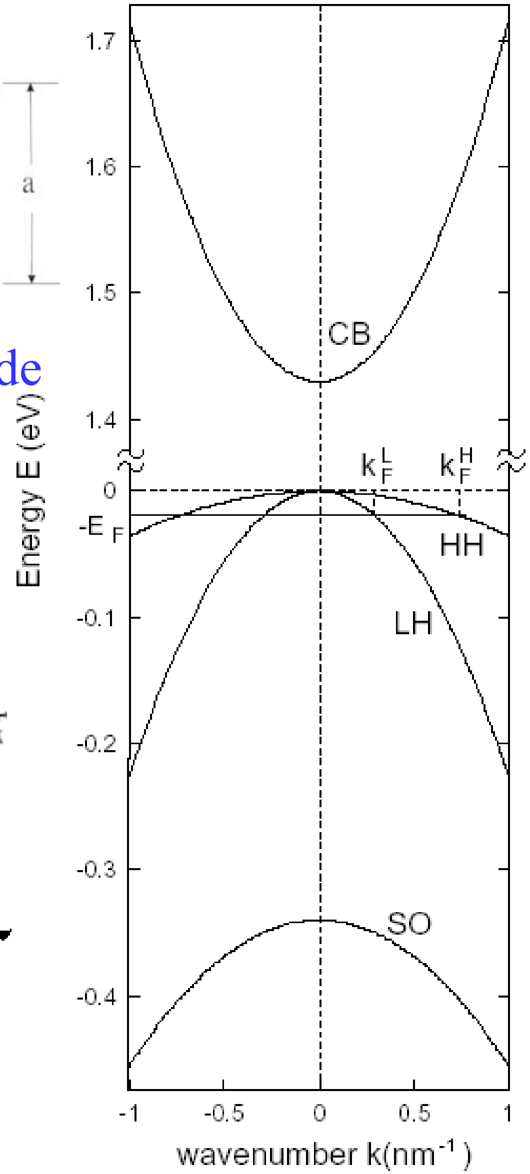

Luttinger model $$H_0 = \frac{\hbar^2}{2m}\left[(\gamma_1 + \frac{5}{2}\gamma_2)k^2 - 2\gamma_2(\vec{k}\cdot\vec{S})^2\right]$$

Equation of motion $$\langle \dot{X}_i \rangle = \frac{\hbar k_i}{m_\lambda} + F_{il}\langle \dot{k}_l \rangle$$

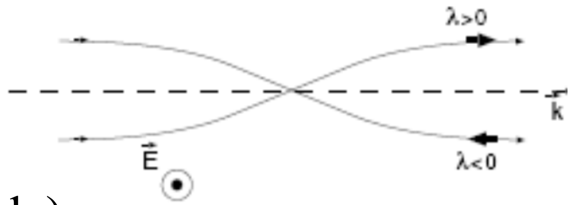

$$\langle \dot{k}_i \rangle = \frac{e}{\hbar}E_i \quad e > 0 \text{ (hole)}$$

Anomalous velocity $$\langle \dot{\vec{X}} \rangle = \frac{\hbar \vec{k}}{m_\lambda} - \frac{e\lambda}{\hbar k^3}\vec{k}\times\vec{E}$$

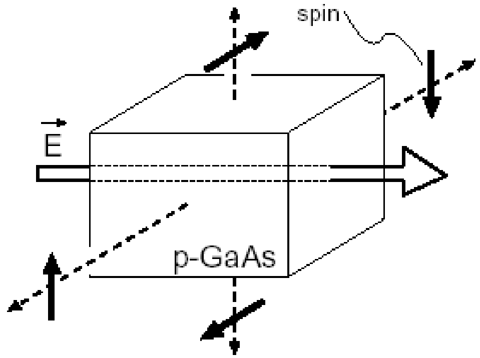

$$j_j^i = \sigma_s \varepsilon^{ijk} E_k$$

$$j_y^x = \frac{eE_z}{12\pi^2}(3k_F^{\mathrm{H}} - k_F^{\mathrm{L}}) = \frac{\hbar}{2e}\sigma_s E_z$$

$n_h = 10^{19}$ cm^{-3}, $\mu = 50$ cm /V·s, $\sigma = e\mu n_h = 80\ \Omega^{-1}\mathrm{cm}^{-1}$;

$\sigma_s = 80\ \Omega^{-1}\mathrm{cm}^{-1}$

First observation of the SHE in n-type 3D GaAs and InGaAs thin films

[Kato *et al.*, Science 306, 1910 (2004)]

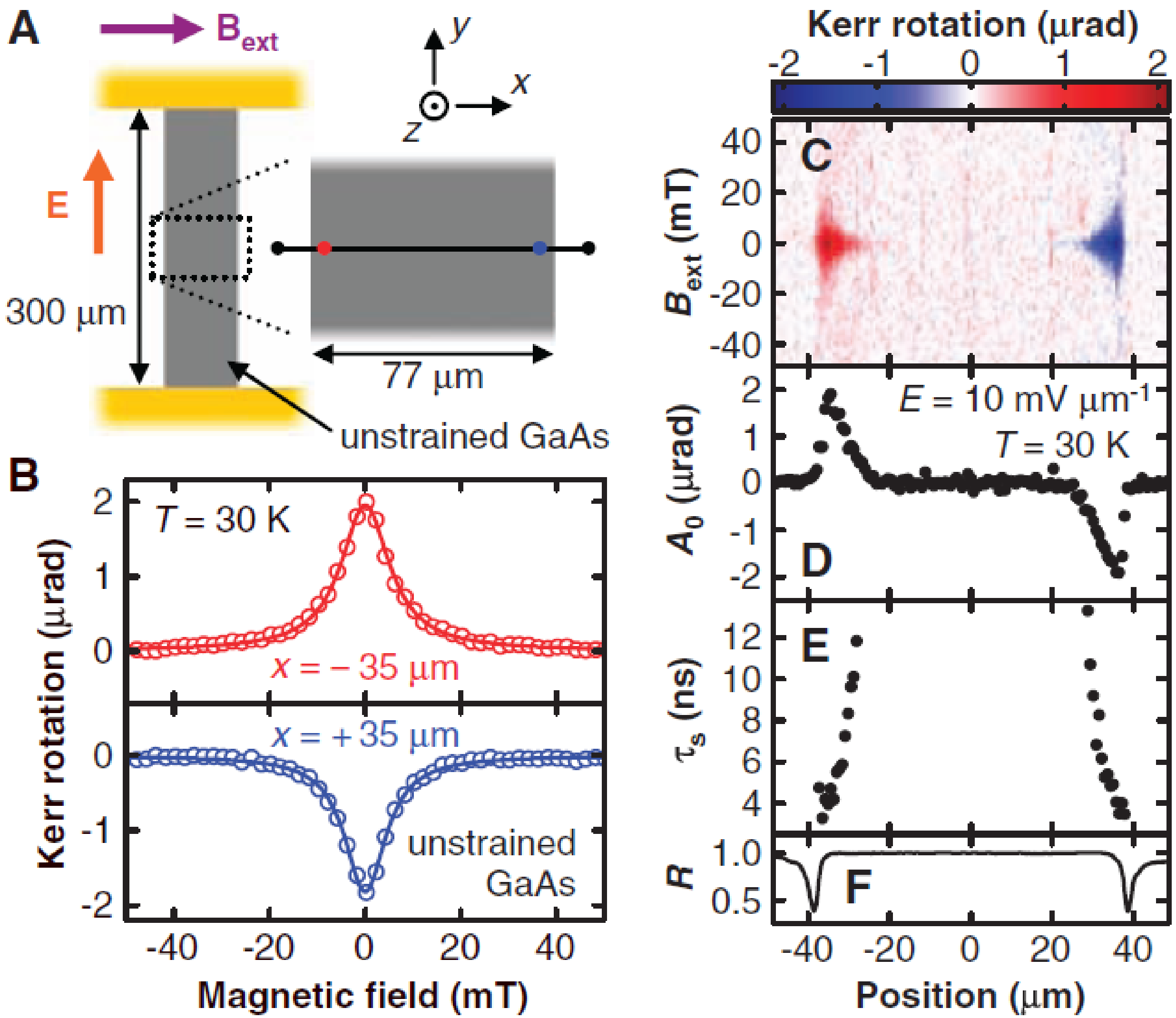

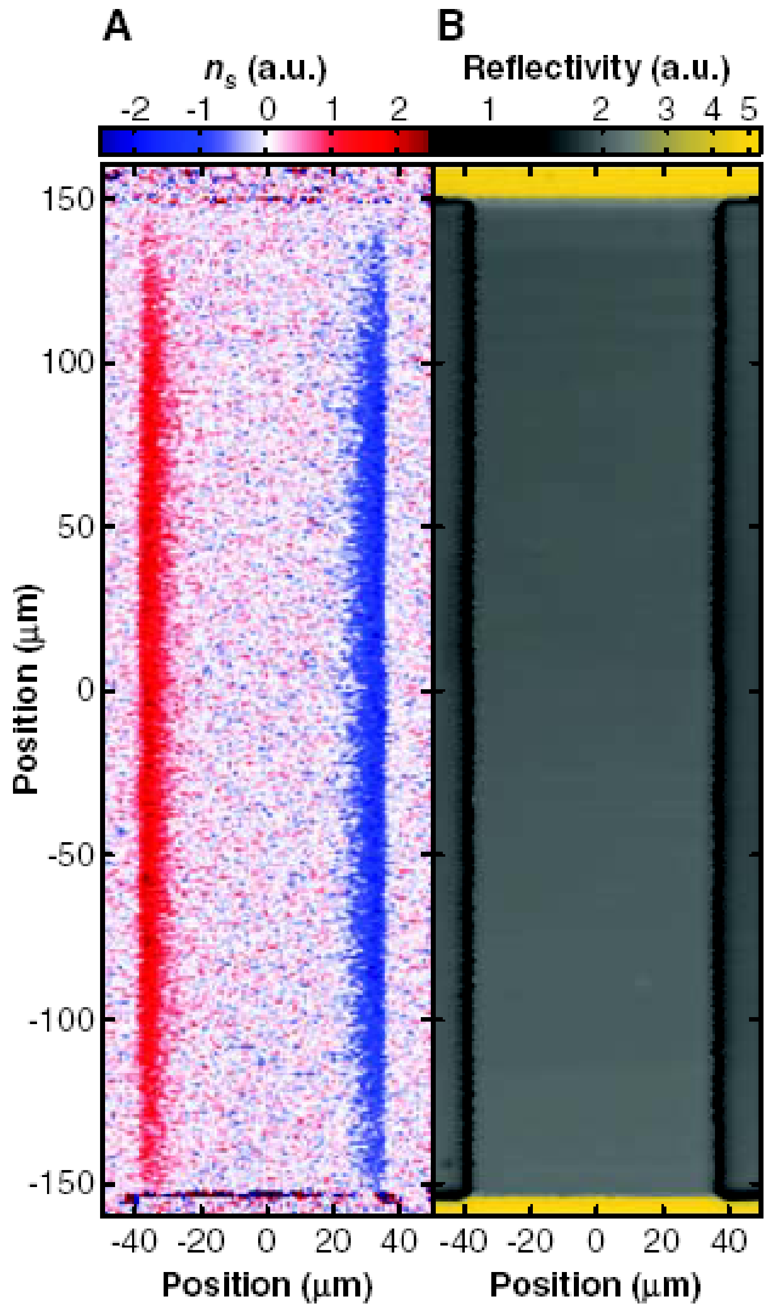

Fig. 2. (**A** and **B**) Two-dimensional images of spin density n_s and reflectivity R, respectively, for the unstrained GaAs sample measured at T = 30 K and E = 10 mV μm^{-1}.

(b) Quantum spin Hall effect and 2D topological insulators

Kane-Mele SOC Hamiltonian for graphene

[Kane & Mele, PRL 95 (2005) 146801; 95 (2005) 226801]

Based on Haldane honeycomb model for QHE without Landau levels [PRL 1998].

$$H_{\mathrm{KM}} = t\sum_{\langle i.\,i\rangle} c_i^{\dagger} c_j + i\lambda \sum_{\langle\langle ij\rangle\rangle} c_i^{\dagger} s_z v_{ij}^{z} c_j$$

$$\mathbf{v}_{ij} = \frac{\mathbf{d}_1 \times \mathbf{d}_2}{\left|\mathbf{d}_1 \times \mathbf{d}_2\right|}$$

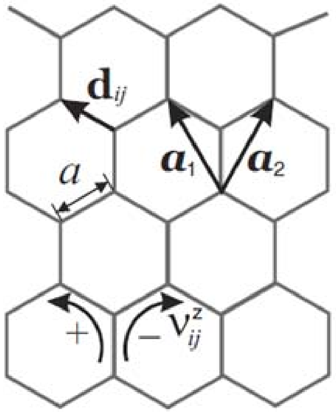

$$\sigma_{xy}^{s} = \left|+1-(-1)\right|\frac{e}{2\pi}, \quad \sigma_{xy} = \left|+1+(-1)\right|\frac{e^2}{h} = 0.$$

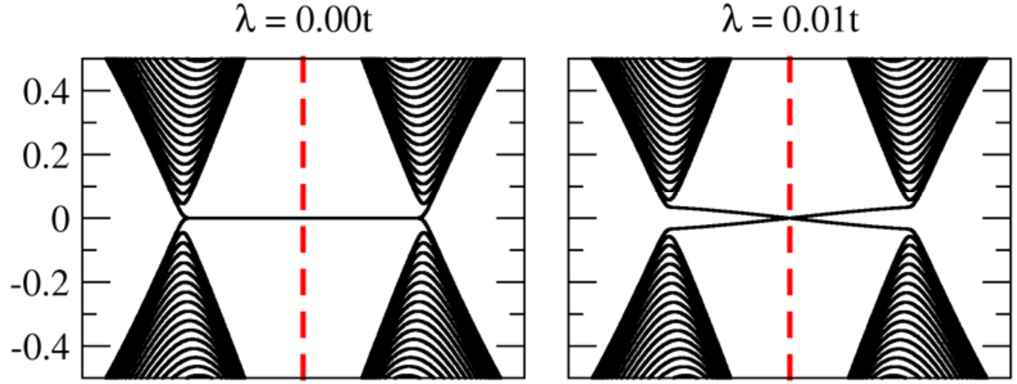

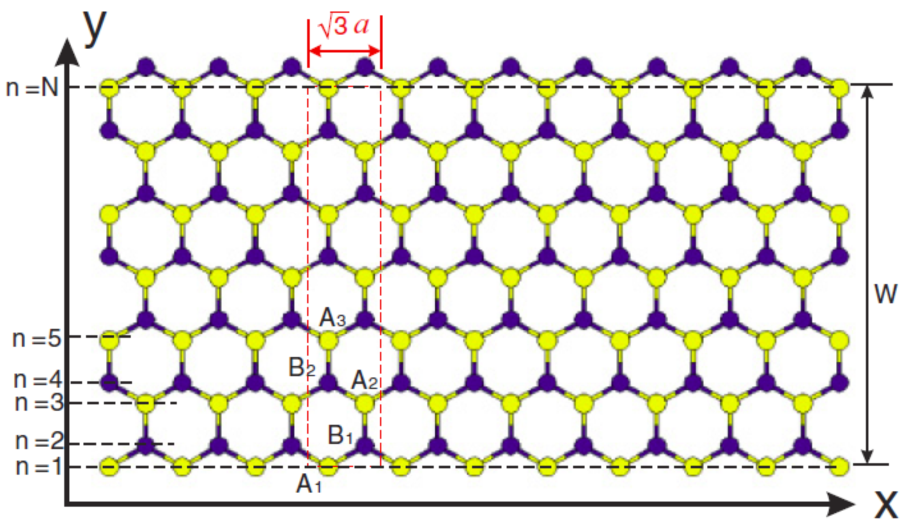

[Chen, Xiao, Chiou, Guo, PRB84 (2011) 165453]

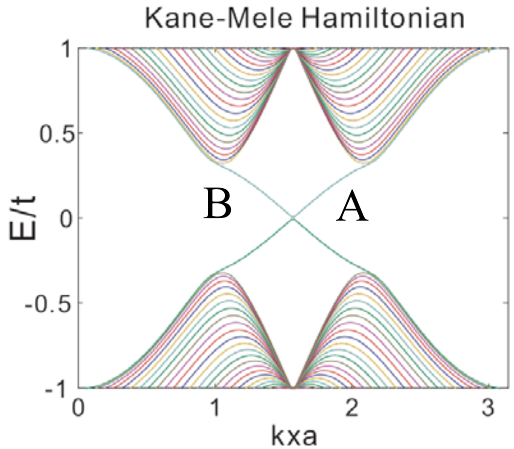

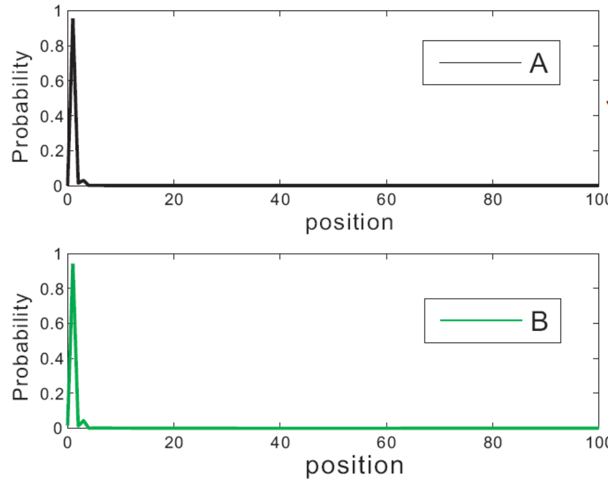

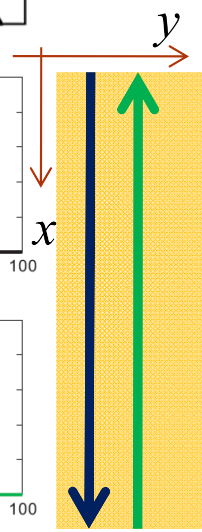

SOC in graphene is too small (<0.01 meV) to make QSHE observable!

Quantum spin Hall effect in semiconductor quantum wells

Quantum spin Hall effect in 2D topological insulator HgTe quantum well

[Bernevig, Hughes, Zhang, Science 314, 1757 (2006)]

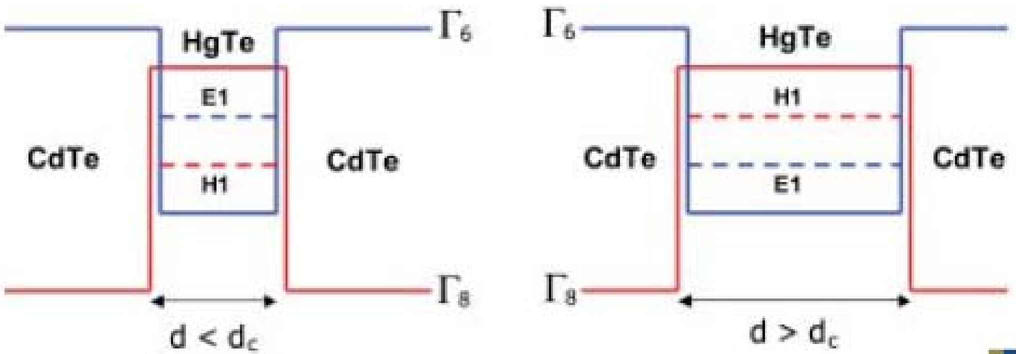

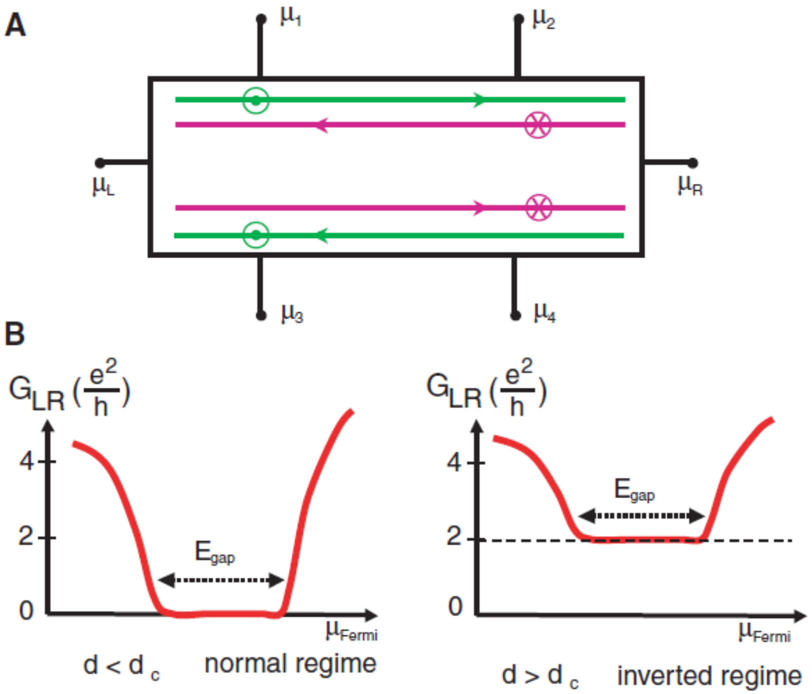

Observation of QSHE in quantum wells

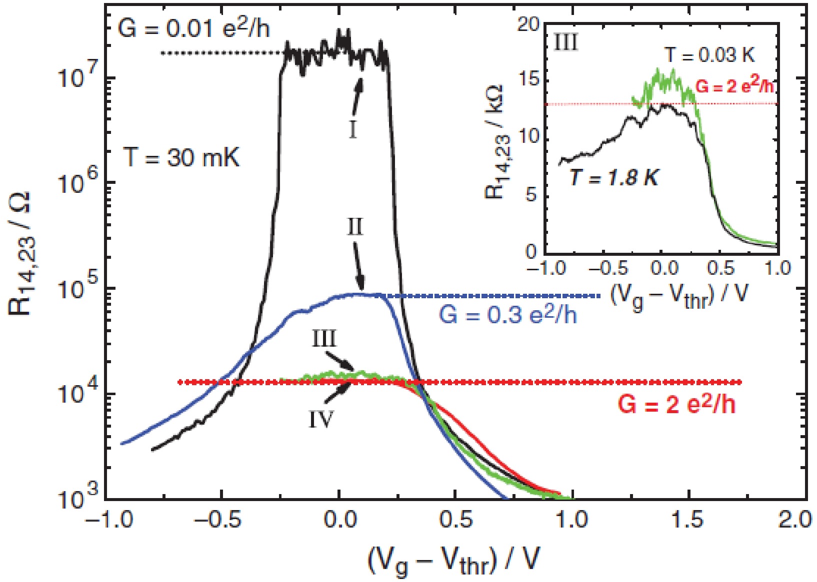

[Koenig et al., Science 318, 766 (2007)]

[Du et al.,PRL 114 (2015) 096802]

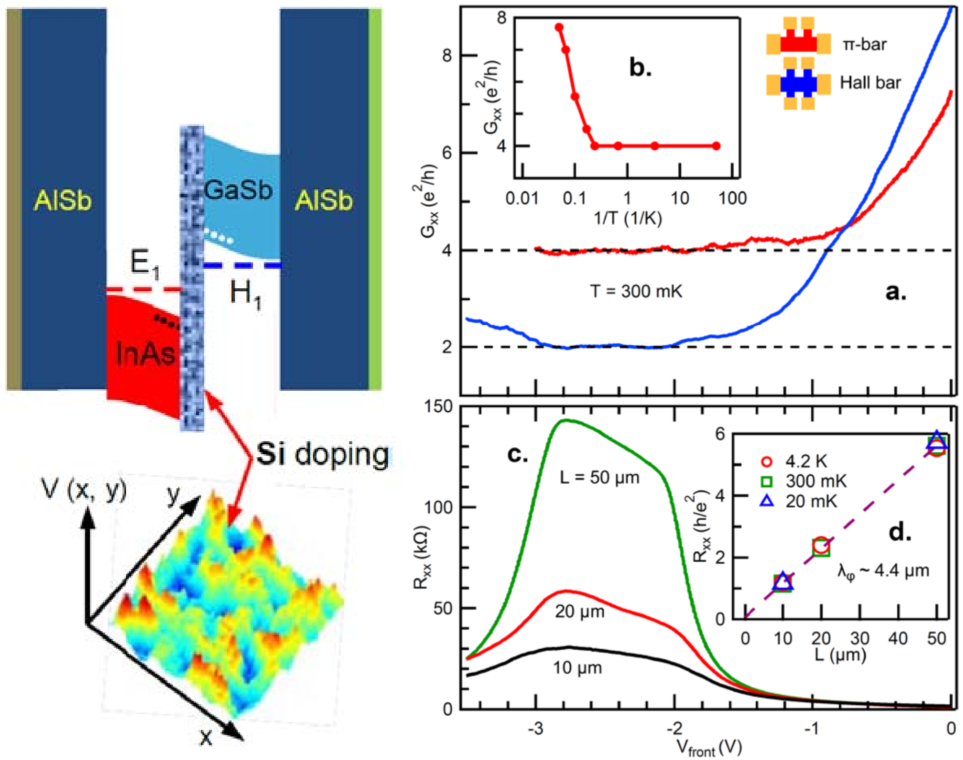

For their pioneering works on topological insulators and quantum spin Hall effect, three theoretical condensed-matter physicists won the 2012 Dirac medal and prize (ICTP in Trieste, Italy)

Shoucheng Zhang (1963 -)

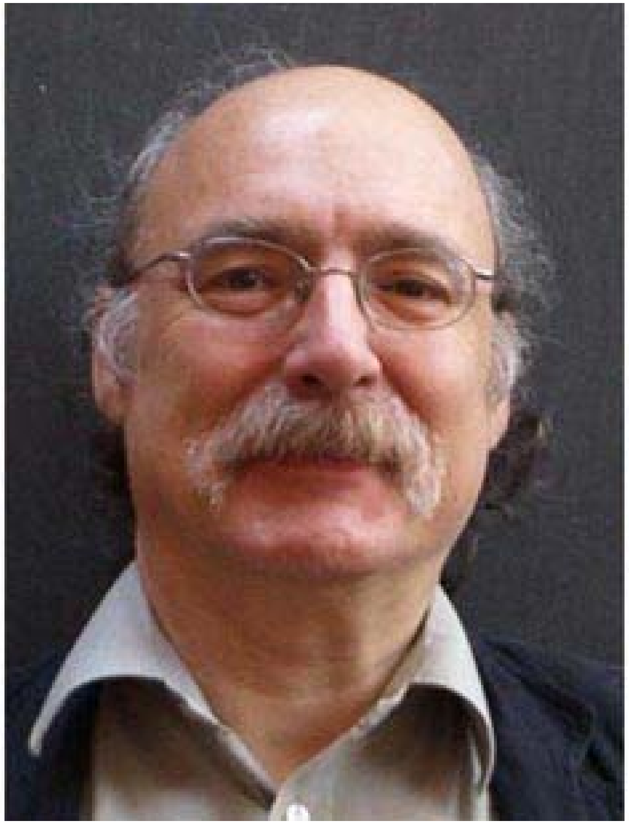

Duncan Haldane (1951 -)

Charles Kane (1963 -)

4) Quantum anomalous Hall effect (QHE without applied magnetic field)

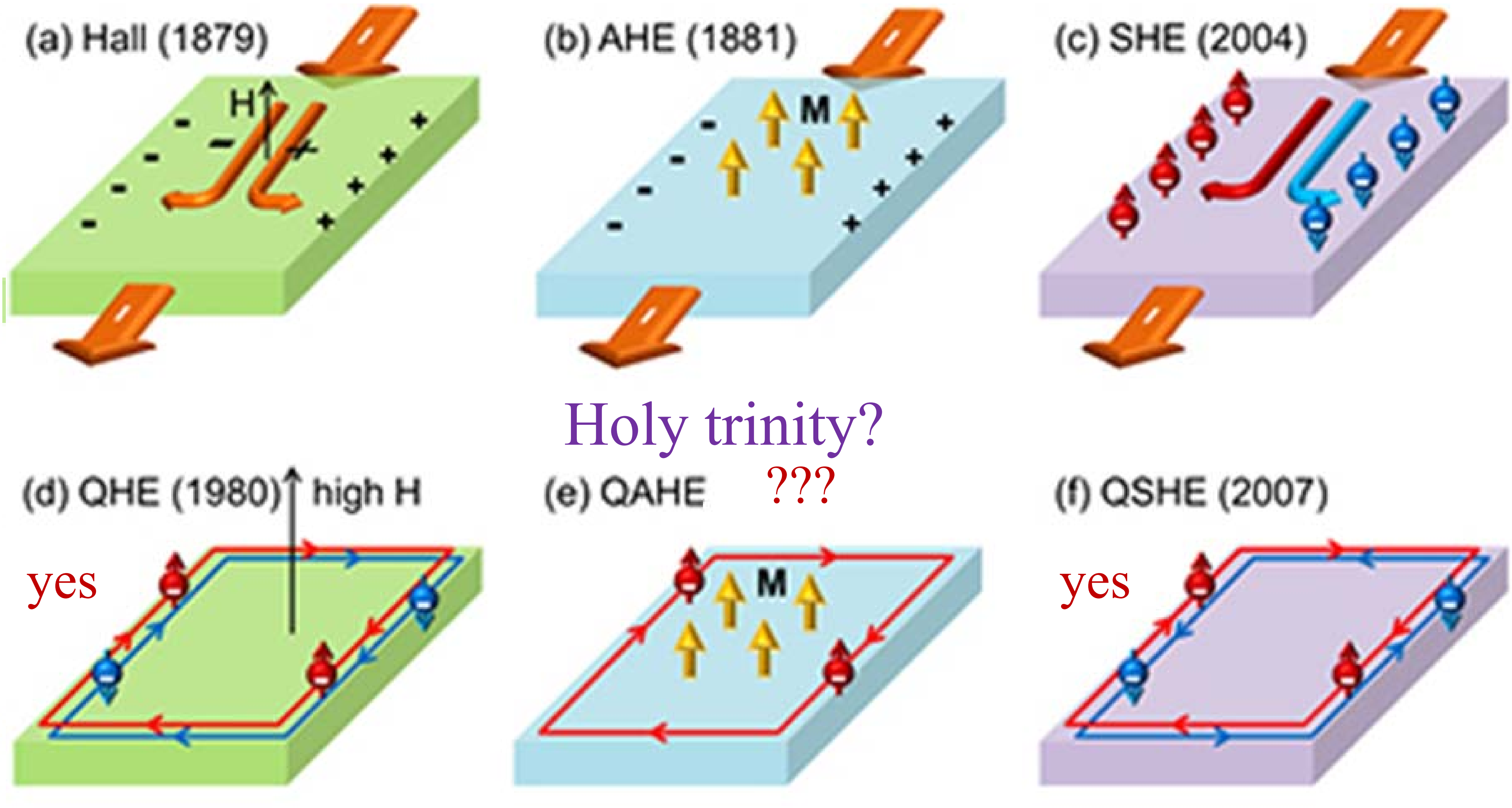

quantum Hall insulator | Chern insulator | topological insulator

Model for a Quantum Hall Effect without Landau Levels: Condensed-Matter Realization of the "Parity Anomaly"

[PRL 61 (1988) 2015]

F. D. M. Haldane

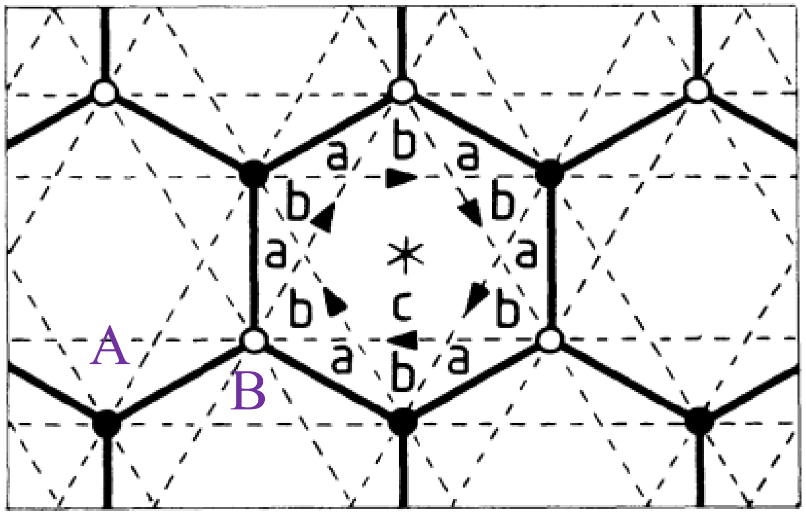

Haldane's 2D honeycomb lattice model (graphene) for spinless electrons

Areas a and b are threaded by fluxes ϕ_a and $\phi_b = -\phi_a$. Area c has no flux. $\phi = 2\pi\,(2\phi_a+\phi_b)/\phi_0$. $\varepsilon_i = \pm 1$.

$$H_H = t_1 \sum_{\langle i,j \rangle} c_i^\dagger c_j + t_2 \sum_{\langle\langle i,j \rangle\rangle} \exp(-i v_{ij}^z \phi) c_i^\dagger c_j + M \sum_i \varepsilon_i c_i^\dagger c_i$$

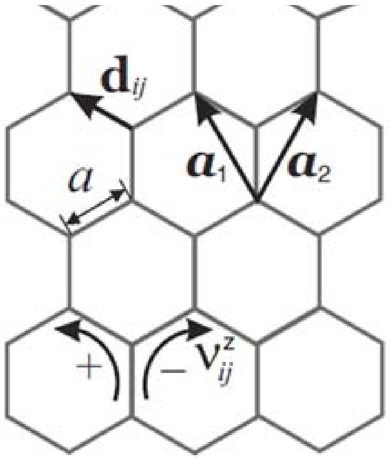

$$v_{ij} = \frac{\mathbf{d}_1 \times \mathbf{d}_2}{|\mathbf{d}_1 \times \mathbf{d}_2|}$$

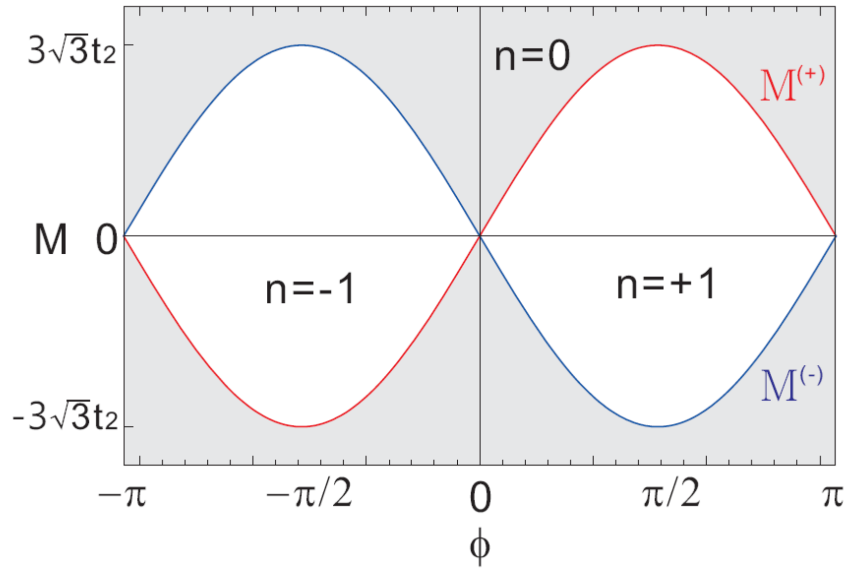

Phase diagram of Haldane model

$[|t_2/t_1| < 1/3]$

If $|M/t_2| < 3\sqrt{3}\,|\sin\phi|$,

$\sigma_{xy} = ne^2/h$.

N.B. Kane-Mele model is two copies of Haldane model with $M = 0$, $\phi = 3\pi/2$ and $\lambda_{SO} = t_2$.

QAHE in real systems: Magnetic impurity-doped topological insulator films

Theoretical proposal:
Bi_2Te_3, Bi_2Se_3 or Sb_2Te_3 films doped with Cr or Fe

[Yu et al., Science 329, 61 (2010)]

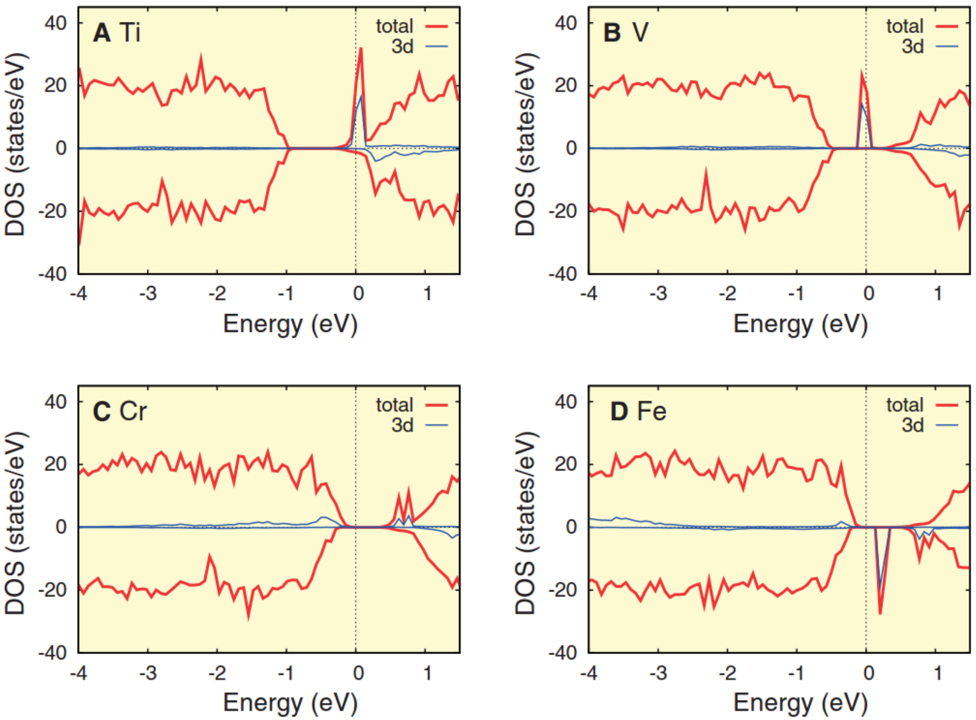

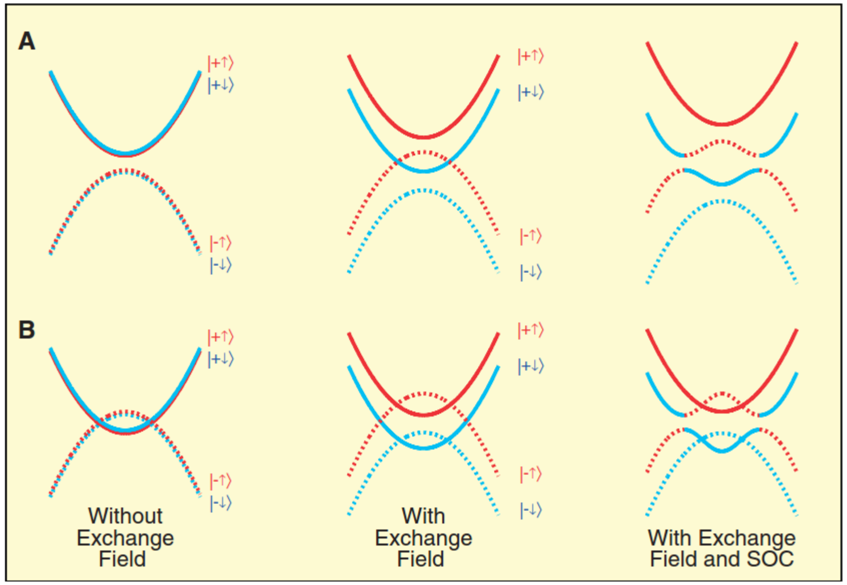

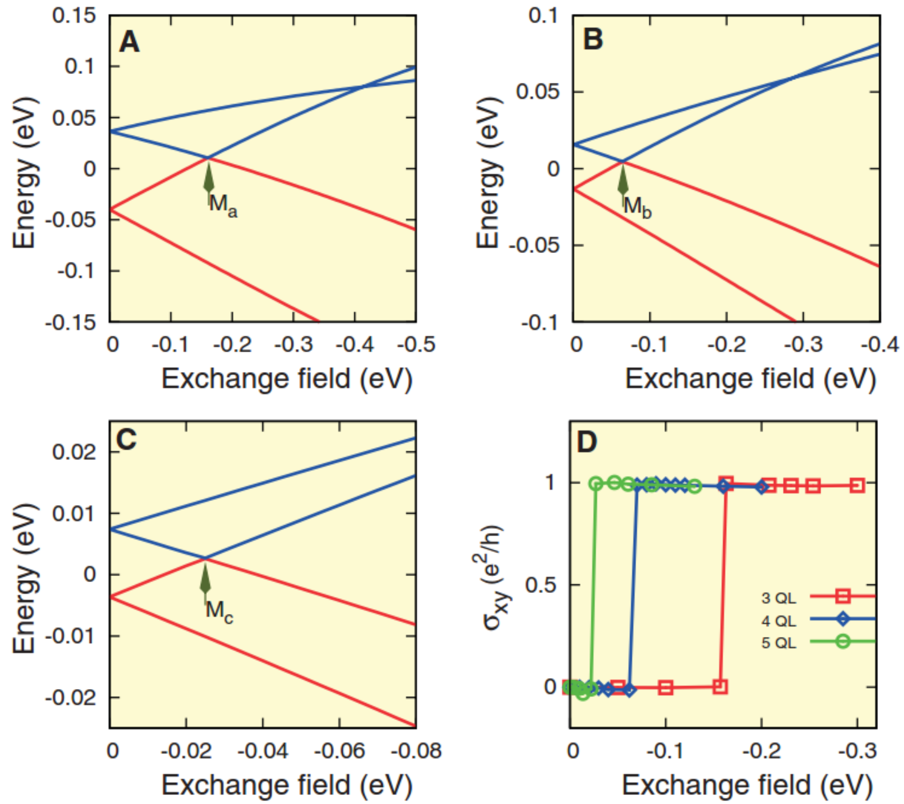

Experimental Observation of the Quantum Anomalous Hall Effect in a Magnetic Topological Insulator

Cui-Zu Chang,[1,2*] Jinsong Zhang,[1*] Xiao Feng,[1,2*] Jie Shen,[2*] Zuocheng Zhang,[1] Minghua Guo,[1] Kang Li,[2] Yunbo Ou,[2] Pang Wei,[2] Li-Li Wang,[2] Zhong-Qing Ji,[2] Yang Feng,[1] Shuaihua Ji,[1] Xi Chen,[1] Jinfeng Jia,[1] Xi Dai,[2] Zhong Fang,[2] Shou-Cheng Zhang,[3] Ke He,[2†] Yayu Wang,[1†] Li Lu,[2] Xu-Cun Ma,[2] Qi-Kun Xue[1†]

First observation on QAHE in $Cr_{0.15}(Bi_{0.1}Sb_{0.9})_{1.85}Te_3$ (5 QLs) thin films

[Science 340, 167 (2013)]

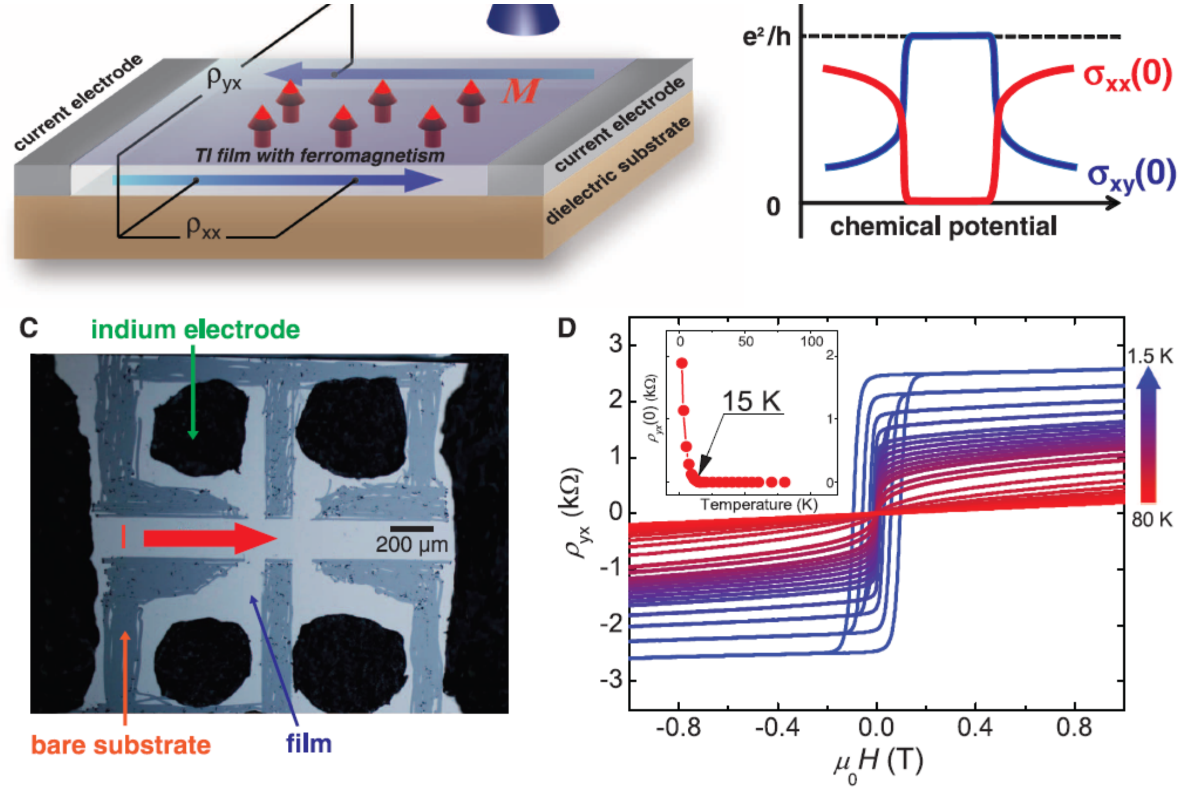

QAHE in $Cr_{0.15}(Bi_{0.1}Sb_{0.9})_{1.85}Te_3$ thin films

[Science 340, 167 (2013)]

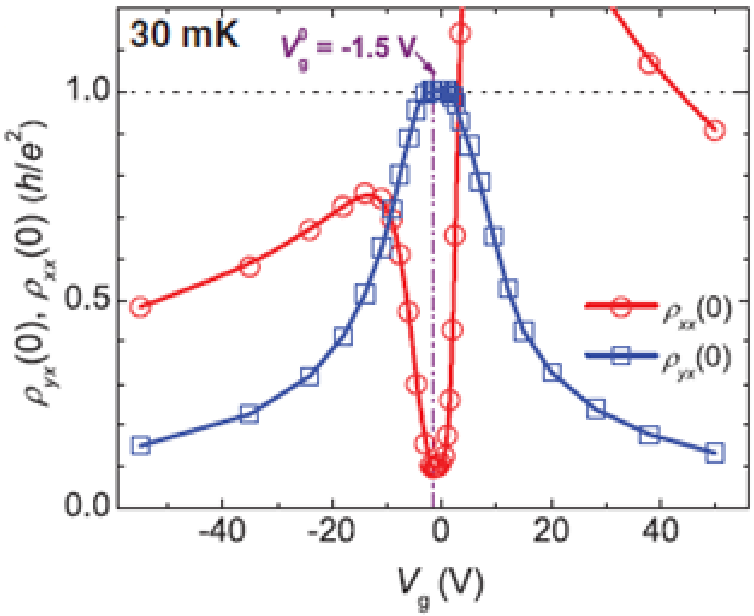

Xue just won the first Future Science Prize ("China's Nobel Prize", US$ 1 million) for his team's observation of the QAHE and also superconductivity in FeSe monolayer/$SrTiO_3$.

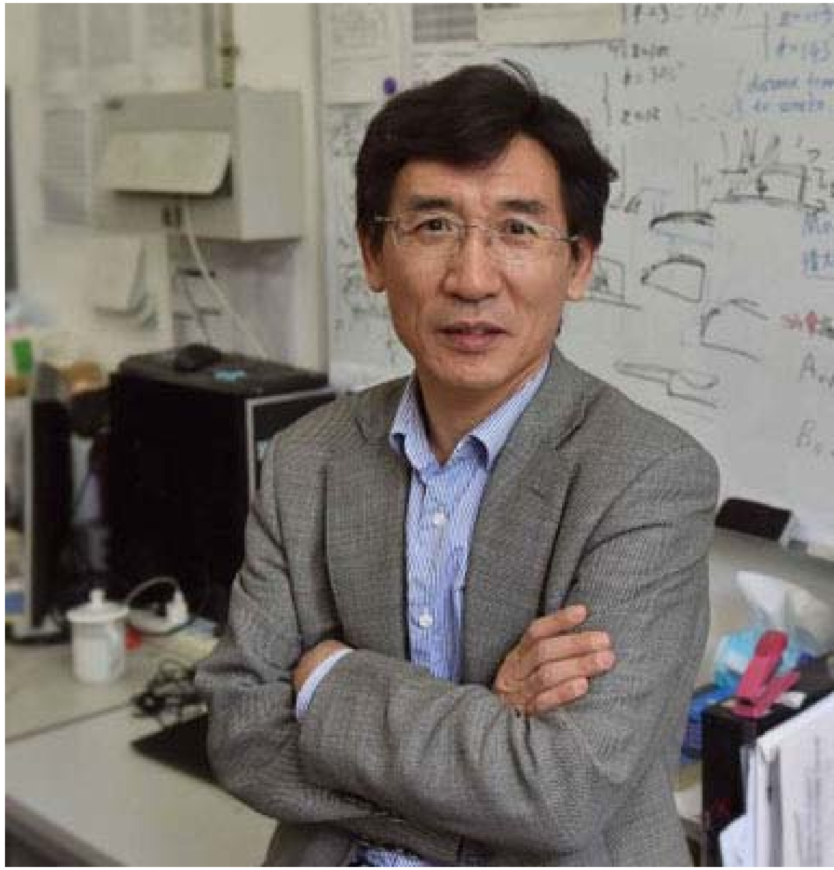

Qikun Xue (1963 -)

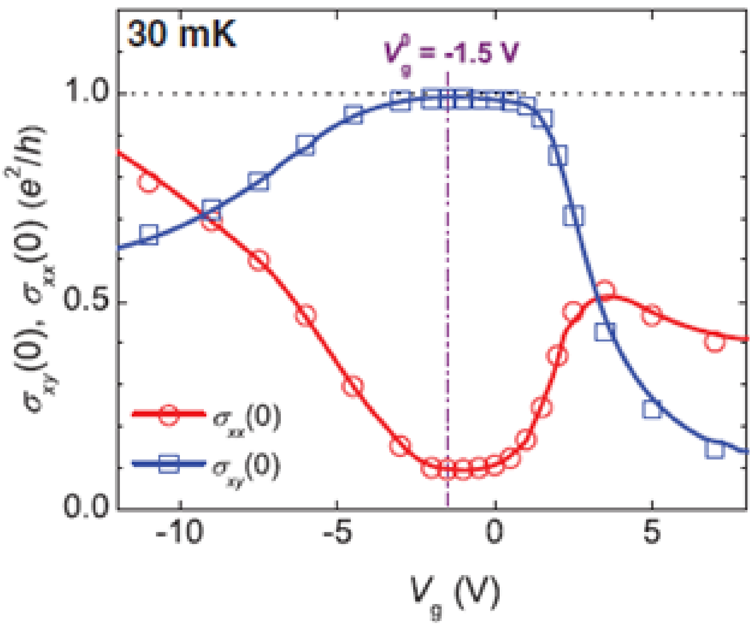

Remaining issues:

QAHE below 30 mK due to

(a) Small band gap (~10 meV);

(b) Weak exchange coupling T_c = ~15 K

(a) Low mobility (760 cm^2/Vs).

3. Why search for SQHE in layered 4d and 5d transition metal oxides

Charge-orbital ordering in Fe_3O_4

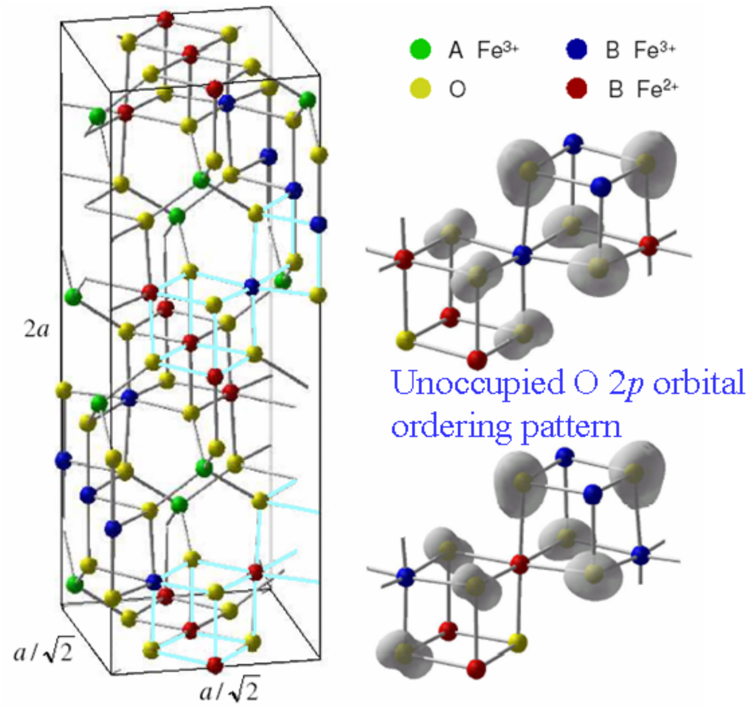

[Jeng, Guo, Huang, PRL 93 (2004) 156403; Huang et al., PRL 96 (2006) 096401]

1) Transition metal oxides

A fascinating family of solid state systems:
high T_c superconductivity: $YBa_2Cu_3O_{6.9}$
colossal magnetoresistance: $La_{2/3}Ca_{1/3}MnO_3$
half-metallicity for spintronics: Sr_2FeMoO_6
ferroelectricity: $BaTiO_3$
charge-orbital ordering: Fe_3O_4

2) Layered 4d and 5d transition metal oxides as Chern insulator candidates

Electron correlations in 3d transition metal oxides are strong, which is challenging to describe, and make them become Mott (trivial) insulators. So far, many-body theory appears unnecessary for TI research.

Layered 4d and 5d transition metal oxides have
stronger SOC (larger band gaps?),
moderate/weak correlation (easier to study?) and
intrinsic itinerant magnetism (higher mobility?).

II. Chern insulator in 4d and 5d transition metal perovskite bilayers

1. 4d and 5d metal perovskite bilayers along [111] direction

Perovskite $(AB'O_3)_N/(ABO_3)_2$ bilayer candidates for a topological insulator

[Xiao et al., NC 2 (2011) 596]

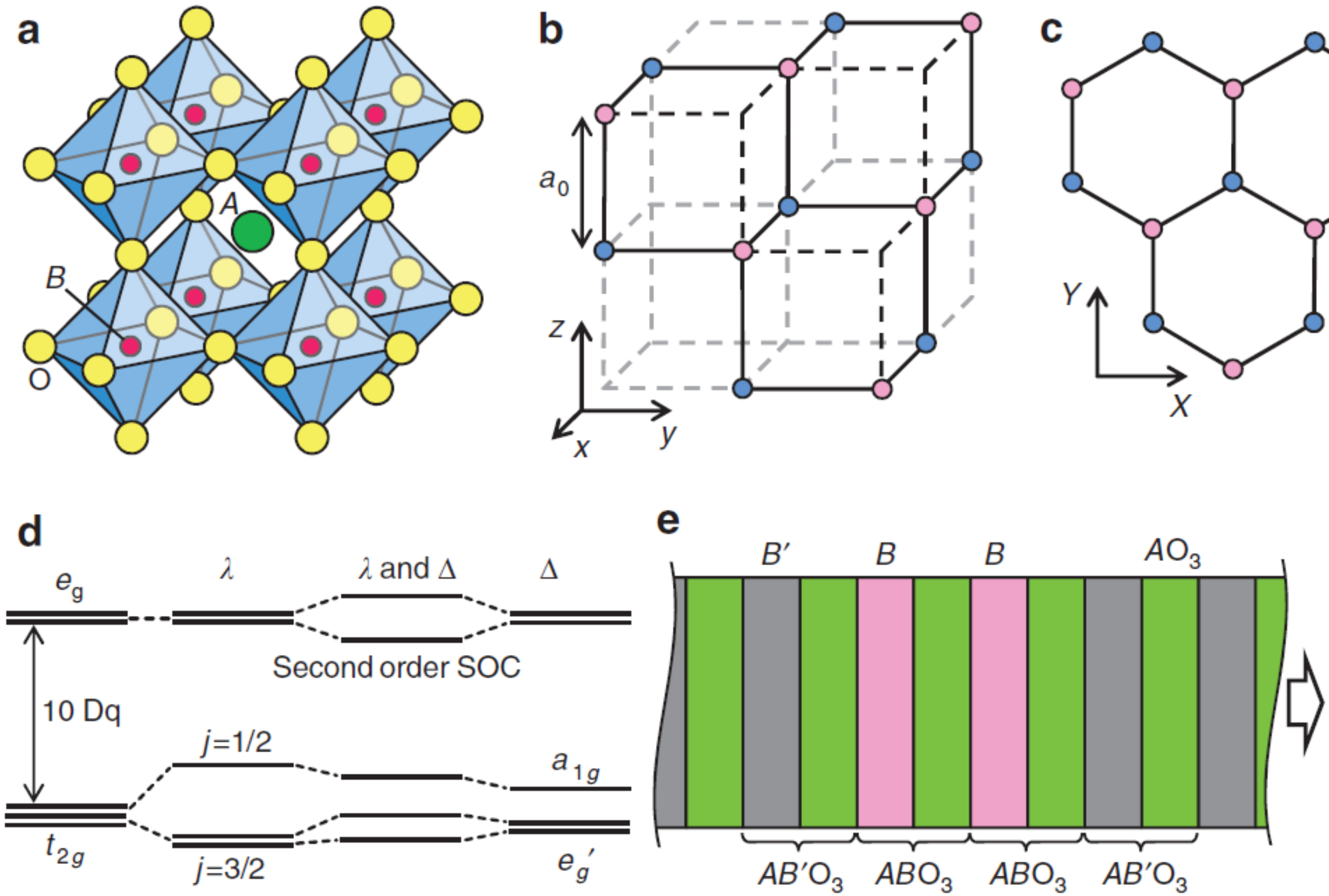

List of ABO_3 candidates.
B' = Al or Ti.

	Conf	bulk
$LaReO_3$	t_{2g}^{4}	--
$LaRuO_3$	t_{2g}^{5}	metallic
$SrRhO_3$	t_{2g}^{5}	metallic
$SrIrO_3$	t_{2g}^{5}	metallic
$LaOsO_3$	t_{2g}^{5}	--
$LaAgO_3$	e_g^{2}	metallic
$LaAuO_3$	e_g^{2}	--

Design principle: Start with a band structure having 'Dirac points' without SOC, and then examine whether a gap opened at those points with the SOC turned on.

Electronic band structure and topology

[Xiao et al., NC 2 (2011) 596]

t_{2g} model: λ/t=5 with Δ/t=1(red) & Δ=0(green)

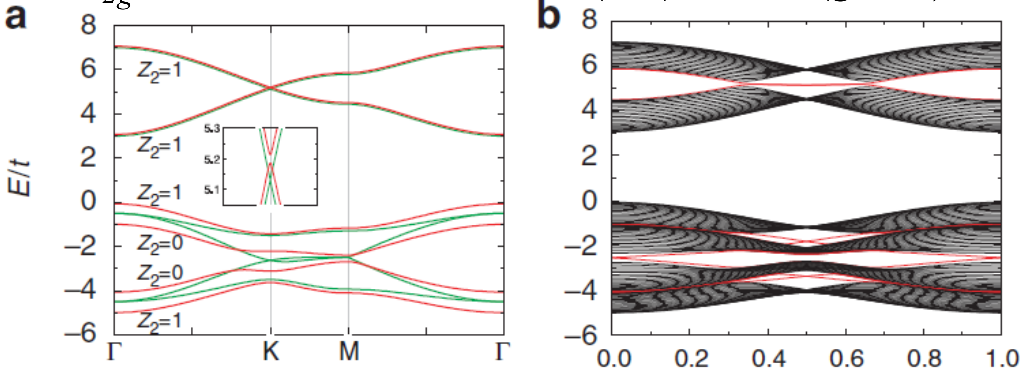

t_{2g} model: Δ/t=0.5, λ/t=1.5 (red) & Δ/t=1.5, λ=0(gree

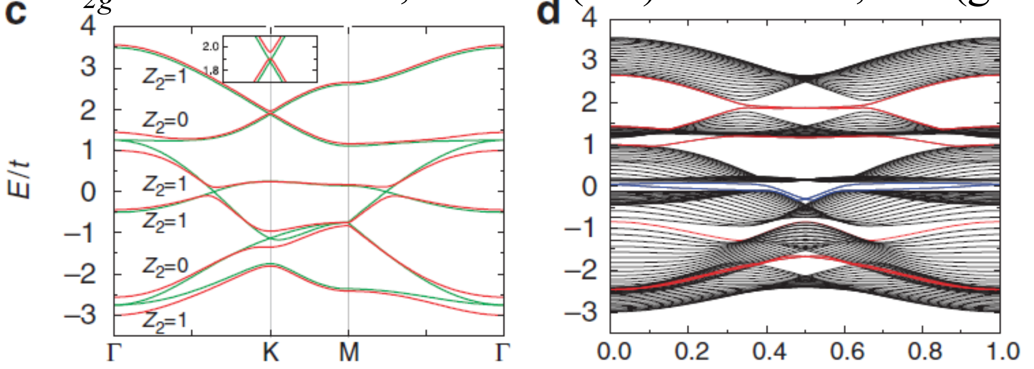

e_g model: λ'/t=0.2 (red) & λ'/t=0(green)

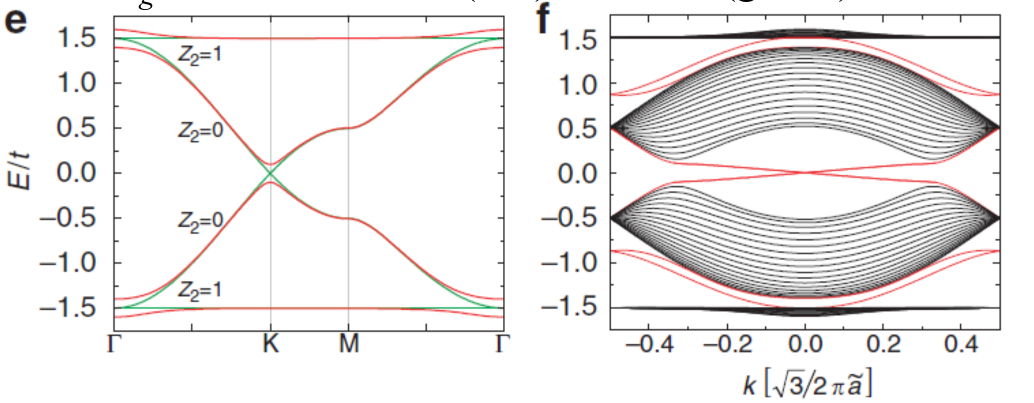

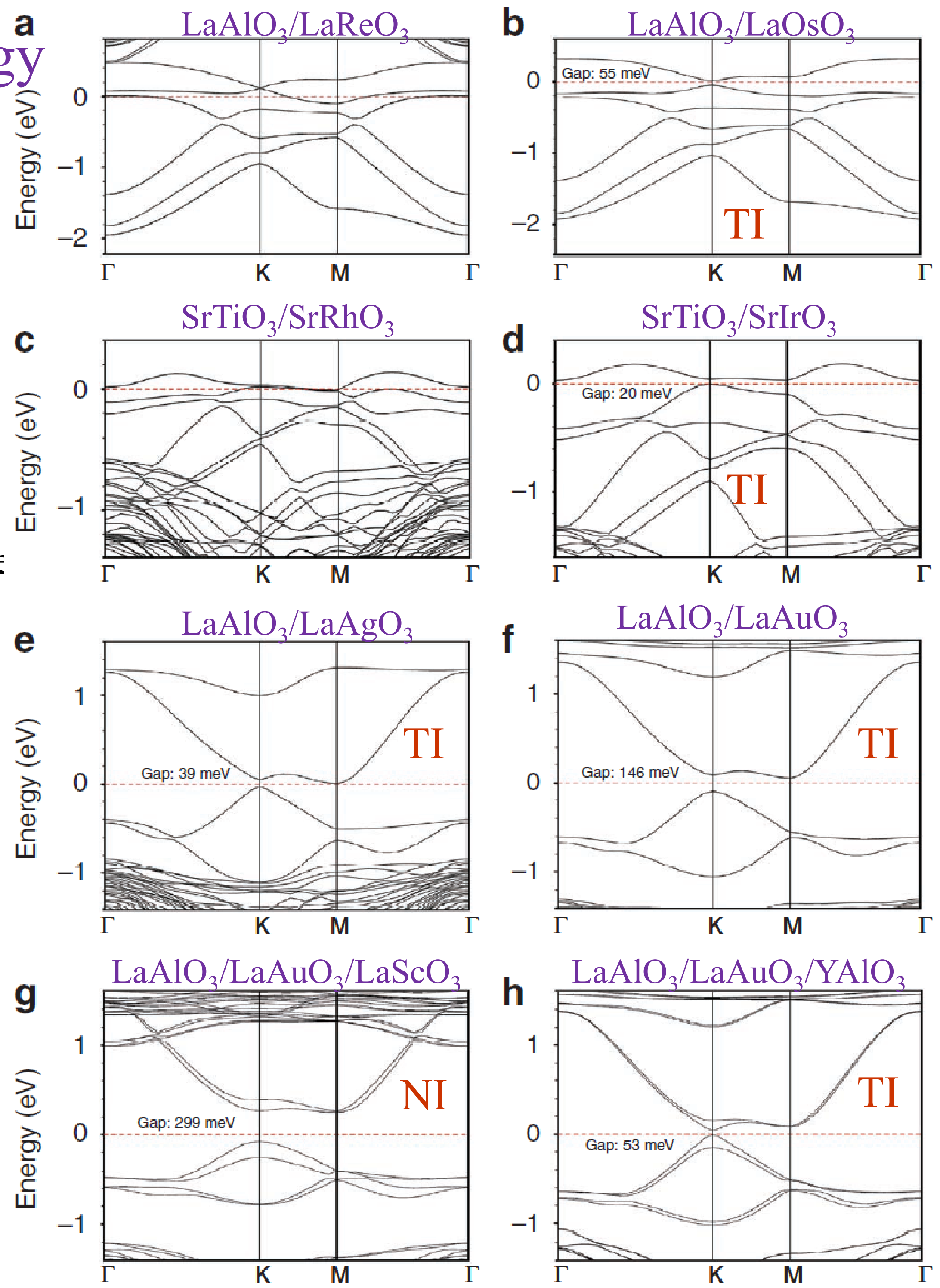

2. Magnetic and electronic properties

[Chandra & Guo, arXiv: 1609.07383 (2016)]

ABO_3	Conf	Bulk	Superlat
$LaRuO_3$	d^5 (t_{2g}^5)	metallic	
$LaAgO_3$	d^8 (e_g^2)	metallic	
$LaReO_3$	d^4 (t_{2g}^4)	metallic*	
$LaOsO_3$	d^5 (t_{2g}^5)	metallic*	
$LaAuO_3$	d^8 (e_g^2)	metallic	
$SrRhO_3$	d^5 (t_{2g}^5)	metallic	yes [6]
$SrAgO_3$	d^7 (e_g^1)	metallic*	
$SrOsO_3$	d^4 (t_{2g}^4)	metallic	
$SrIrO_3$	d^5 (t_{2g}^5)	metallic	Yes [10]

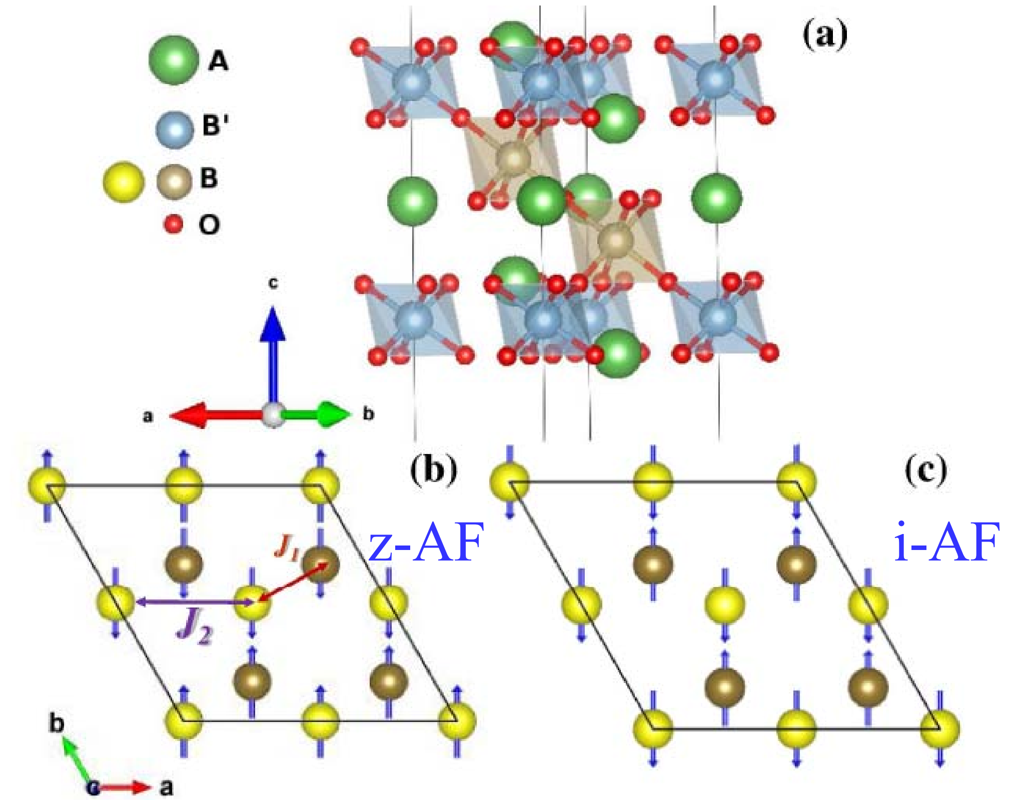

*

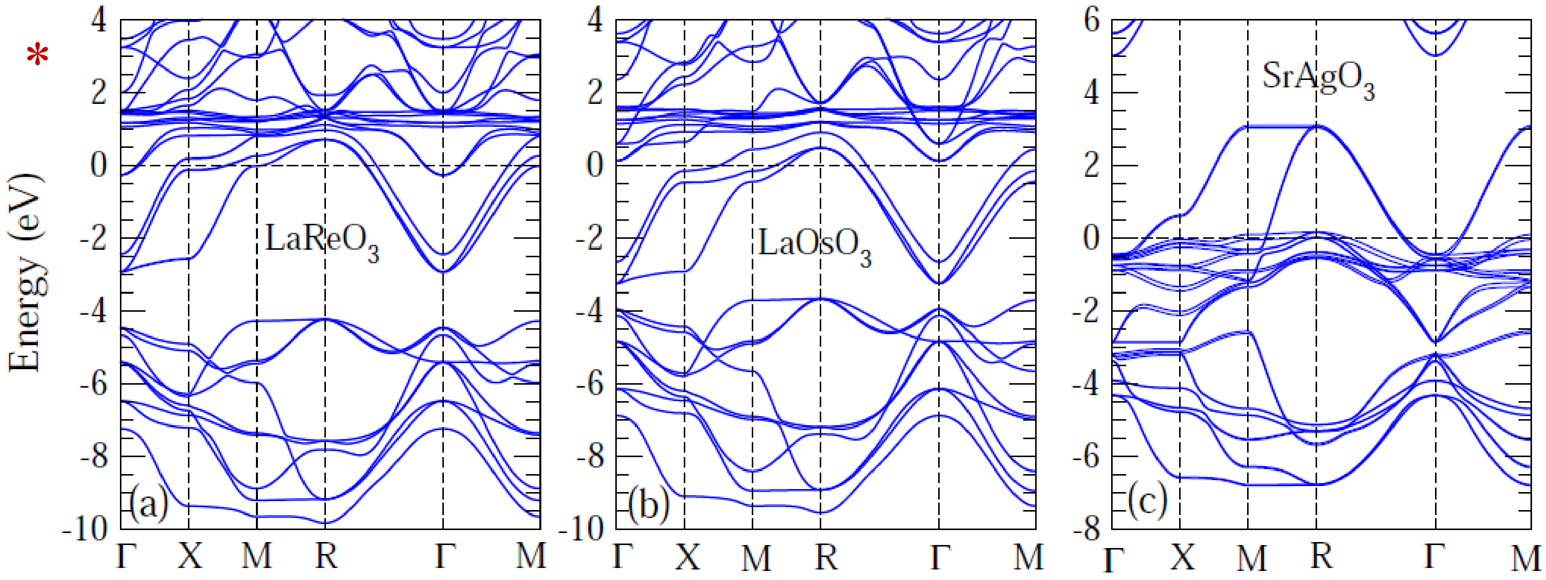

$(ABO_3)_2/(AB'O_3)_{10}$ superlattices

$AB'O_3 = LaAlO_3$ or $SrTiO_3$

Physical properties of the magnetic perovskite bilayers

[Chandra & Guo, arXiv: 1609.07383 (2016)]

Bilayer	J_1/J_2 (meV)	T_c (K)	m_s^t (μ_B/cell)	m_s^B (μ_B/atom)	ΔE_{ma} (meV/cell)	E_g (meV)	$N(E_F)$ (states/eV/cell)	P	σ_{xy}^A (e^2/hc)
$(LaRuO_3)_2$	25.6/0.6	311	1.94 (2.00)	0.70	2.4	0	10.41	-0.98 (-1.00)	1.22
$(LaReO_3)_2$	2.4/1.2	56	0.92 (1.49)	0.33	-0.20	0	12.01	-0.08 (0.56)	1.78
$(LaOsO_3)_2$	22.1/1.7	296	0.83 (2.00)	0.30	2.5	38	-	- (-1.00)	2.00
$(SrRhO_3)_2$	20.6/2.0	285	1.89 (2.00)	0.54	-1.8	0	7.98	-0.93 (-1.00)	1.84
$(SrOsO_3)_2$	15.9/4.0	277	2.66 (3.88)	0.81	2.1	0	17.25	0.18 (0.78)	1.52
$(SrIrO_3)_2$	18.7/2.0	263	0.16 (2.00)	0.06	∞	0	1.00	0.27 (-1.00)	0.26

Heisenberg model

$$E = E_0 - \sum_{i<j} J_{ij} \sigma_i \cdot \sigma_j$$

Mean-field estimation

$$k_B T_C = \frac{1}{3} \sum_j J_{0j}$$

*Large exchange couplings, thus high Curie temperatures;

*$(LaOsO_3)_2/(LAO)_{10}$ is an insulator, others, metallic.

*$(LaRuO_3)_2/(LAO)_{10}$ and $(SrRhO_3)_2/(STO)_{10}$, half-metallic;

*Large anomalous Hall conductivities.

Band structure of the magnetic perovskite bilayers

[Chandra & Guo, arXiv: 1609.07383 (2016)]

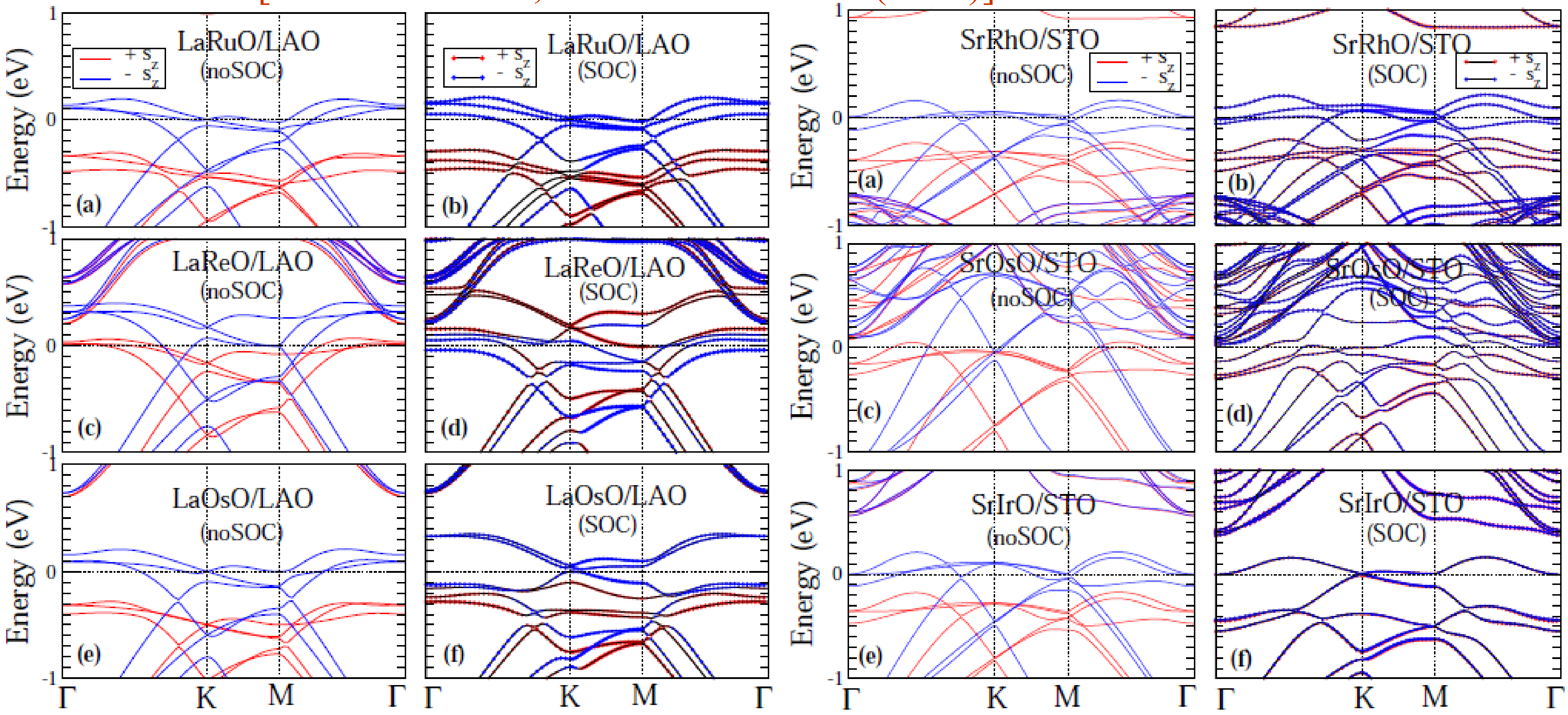

$(LaOsO_3)_2/(LAO)_{10}$ is an insulator with a gap of 38 meV,
$(SrIrO_3)_2/(STO)_{10}$ is a semimetal and the rest are metallic.
$(LaRuO_3)_2/(LAO)_{10}$ and $(SrRhO_3)_2/(STO)_{10}$ are half-metallic.

Quantum confinement of conduction electrons

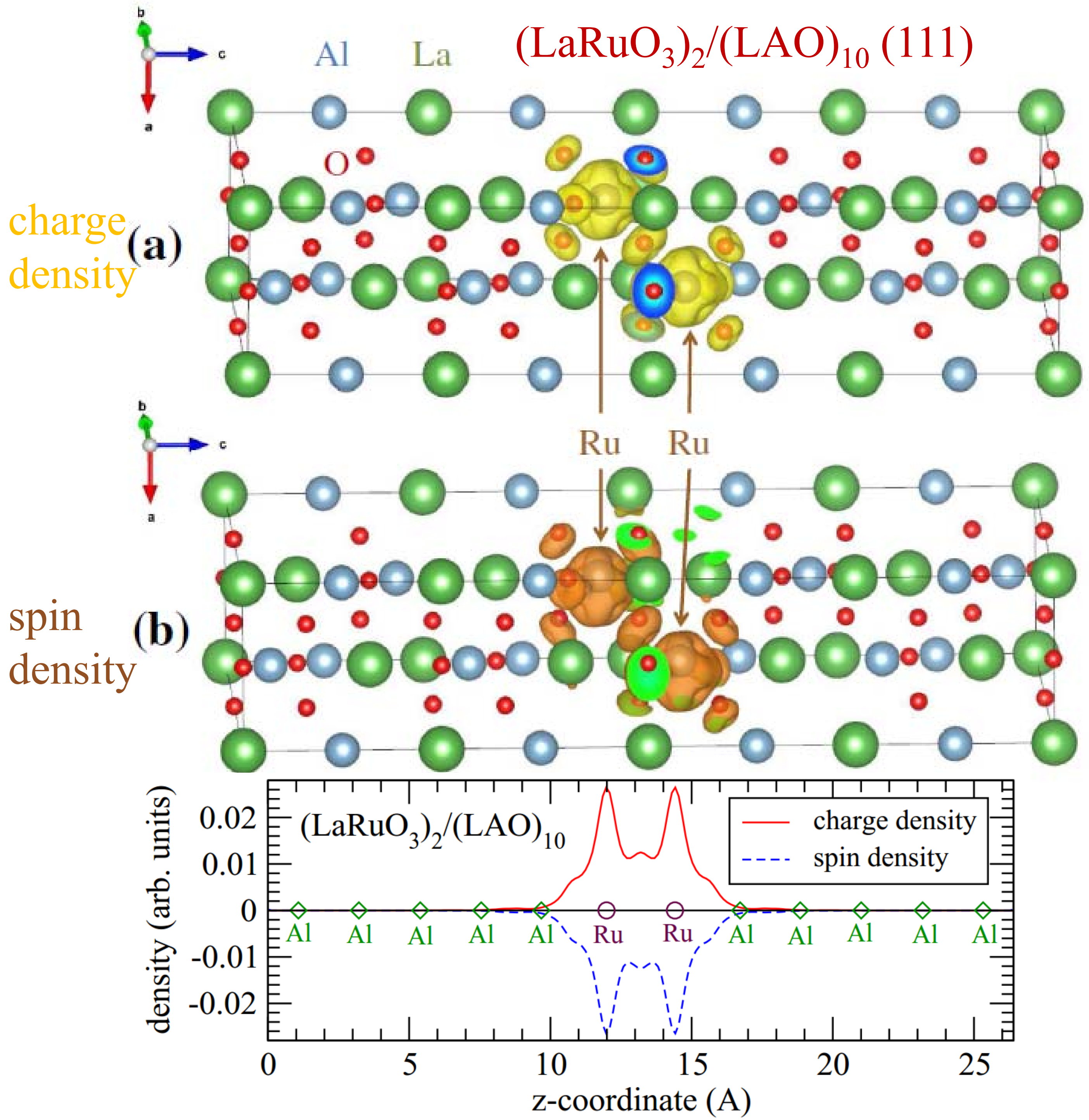

Both charge and spin densities are confined within the $(LaRuO_3)_2$ bilayer in the central part of the superlattice. Although many 3D bulk magnetic materials have been predicted to be half-metallic, quasi-2D fully spin-polarized electron gas systems have been rare.

3. Quantum anomalous Hall phase [Chandra & Guo, arXiv: 1609.07383 (2016)]

$$\sigma_{AH} = -\frac{e^2}{\hbar(2\pi)^3}\int d^3k \sum_n f(\varepsilon_n(\mathbf{k}))\Omega_n^z(\mathbf{k}), \quad \Omega_n^z(\mathbf{k}) = -\sum_{n'\neq n} \frac{2\,\mathrm{Im}\langle \mathbf{k}n|v_x|\mathbf{k}n'\rangle\langle \mathbf{k}n'|v_y|\mathbf{k}n\rangle}{(\omega_{\mathbf{k}n}-\omega_{\mathbf{k}n'})^2}$$

is calculated using the maximally localized Wannier functions fitted to GGA band structure.

For a 3D Chern insulator, $\sigma_{AH} = n_c \frac{e^2}{hc}$, n_c is an integer (Chern number)

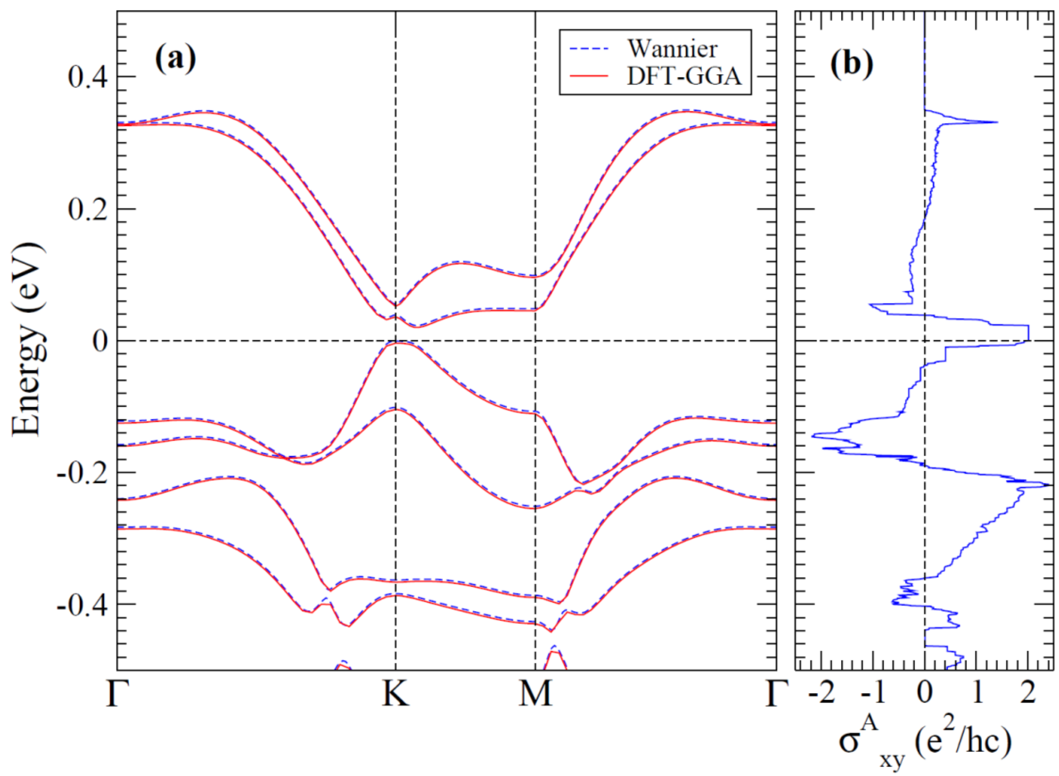

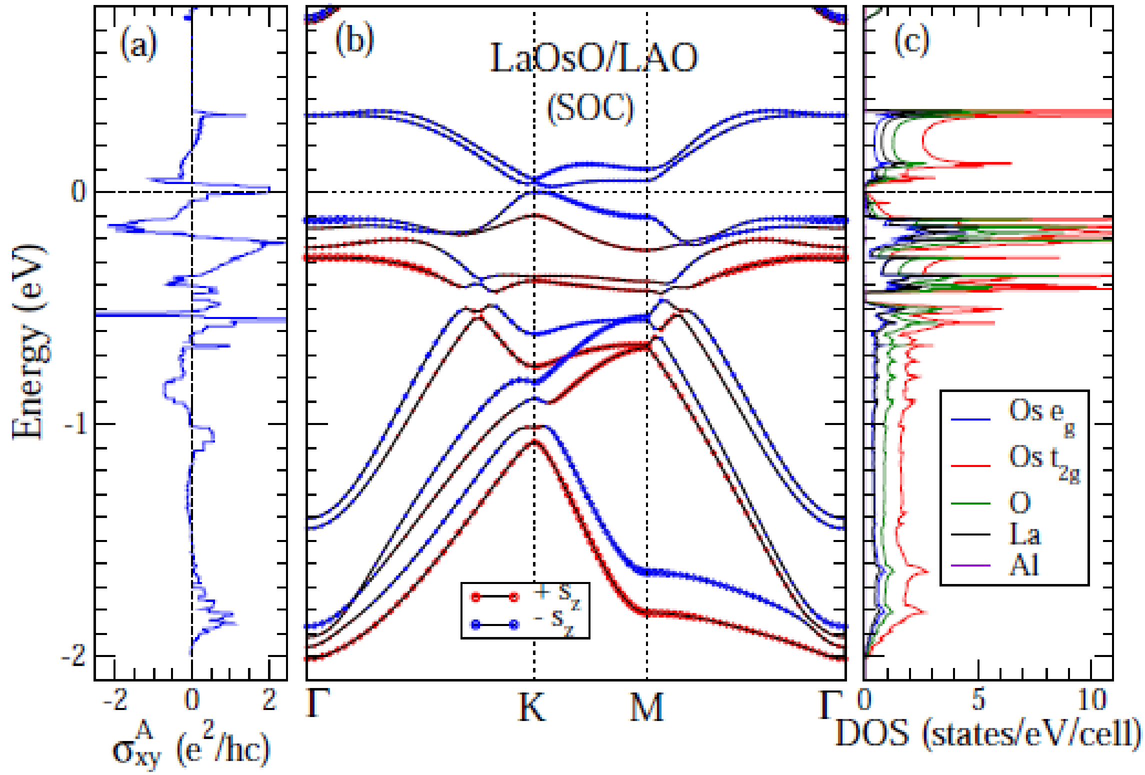

$(LaOsO_3)_2/(LAO)_{10}$ is a spin-polarized quantum anomalous Hall (Chern) insulator (Chern number = 2) with the spin-polarized edge current tunable by applied magnetic field.

III. Quantum topological Hall effect in $K_{1/2}RhO_2$

1. Physical properties of layered oxide K_xRhO_2

1) Crystal structure: [Shibasaki et al., JPCM 22 (2010) 115603]

Layered hexagonal γ-Na_xCoO_2-type structure ($P6_3/mmc$; No. 194) with two CdI_2-type (1T) RhO_2 layers stacked along c-axis [2f.u./cell].

2) Interesting properties:

It is isostructural and also isoelectronic to thermoelectric and superconducting material Na_xCoO_2.

It shows significant thermopower and Seebeck coefficient, and is also expected to become superconducting at low temperatures.

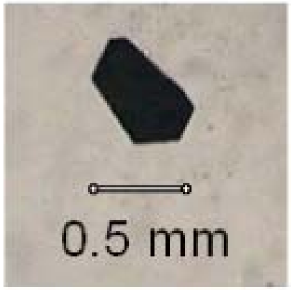

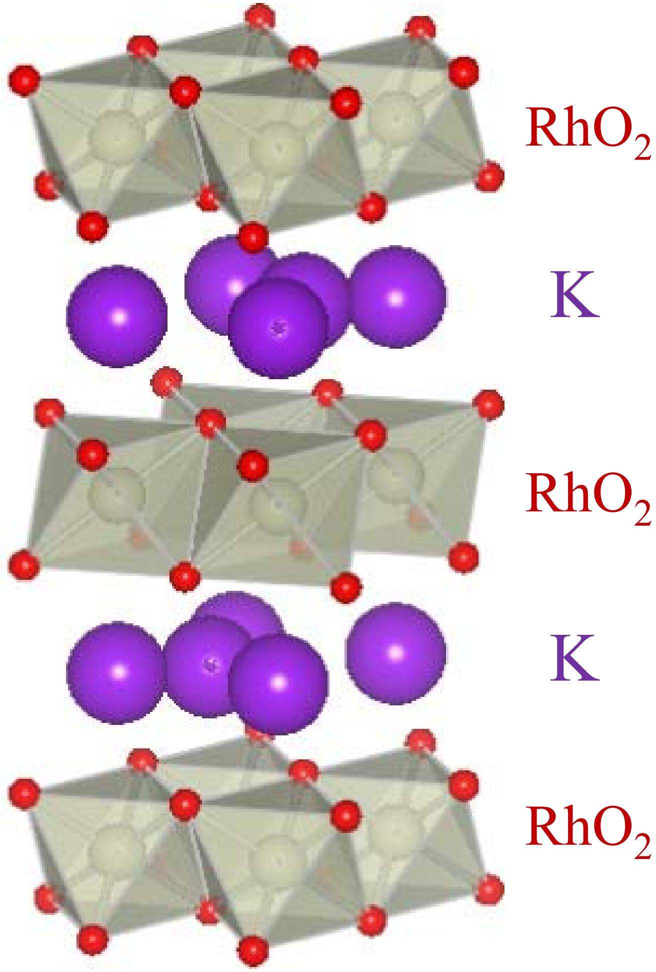

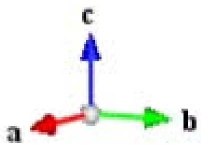

2. Non-coplanar antiferromagnetic ground state structure

1) Energetics of various magnetic structures in $K_{0.5}RhO_2$

[Zhou et al., PRL 116, 256601 (2016)]

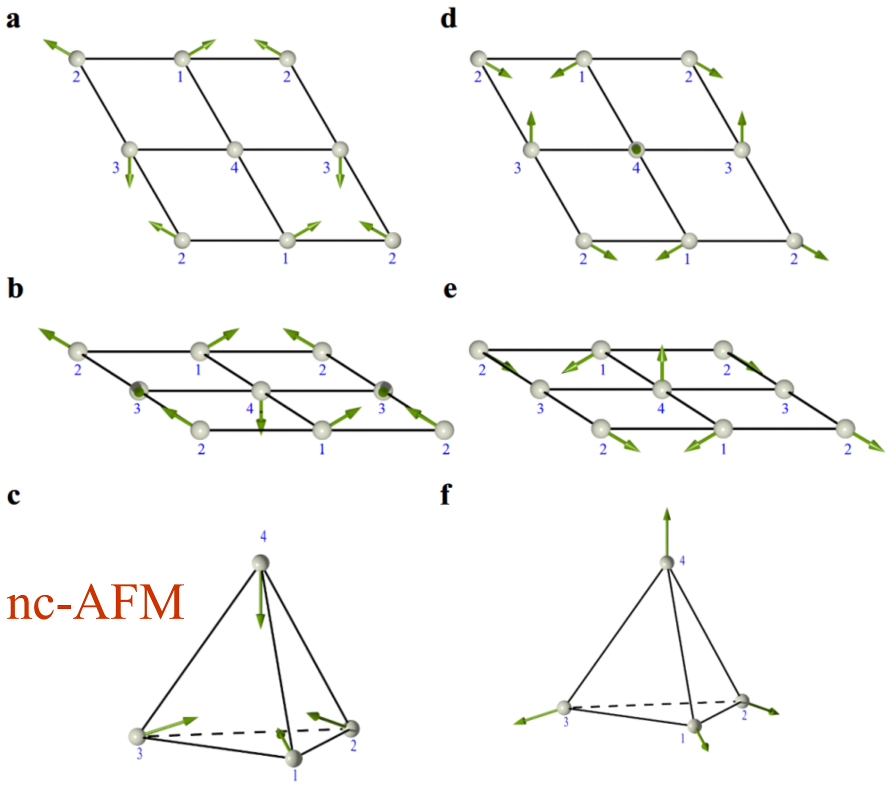

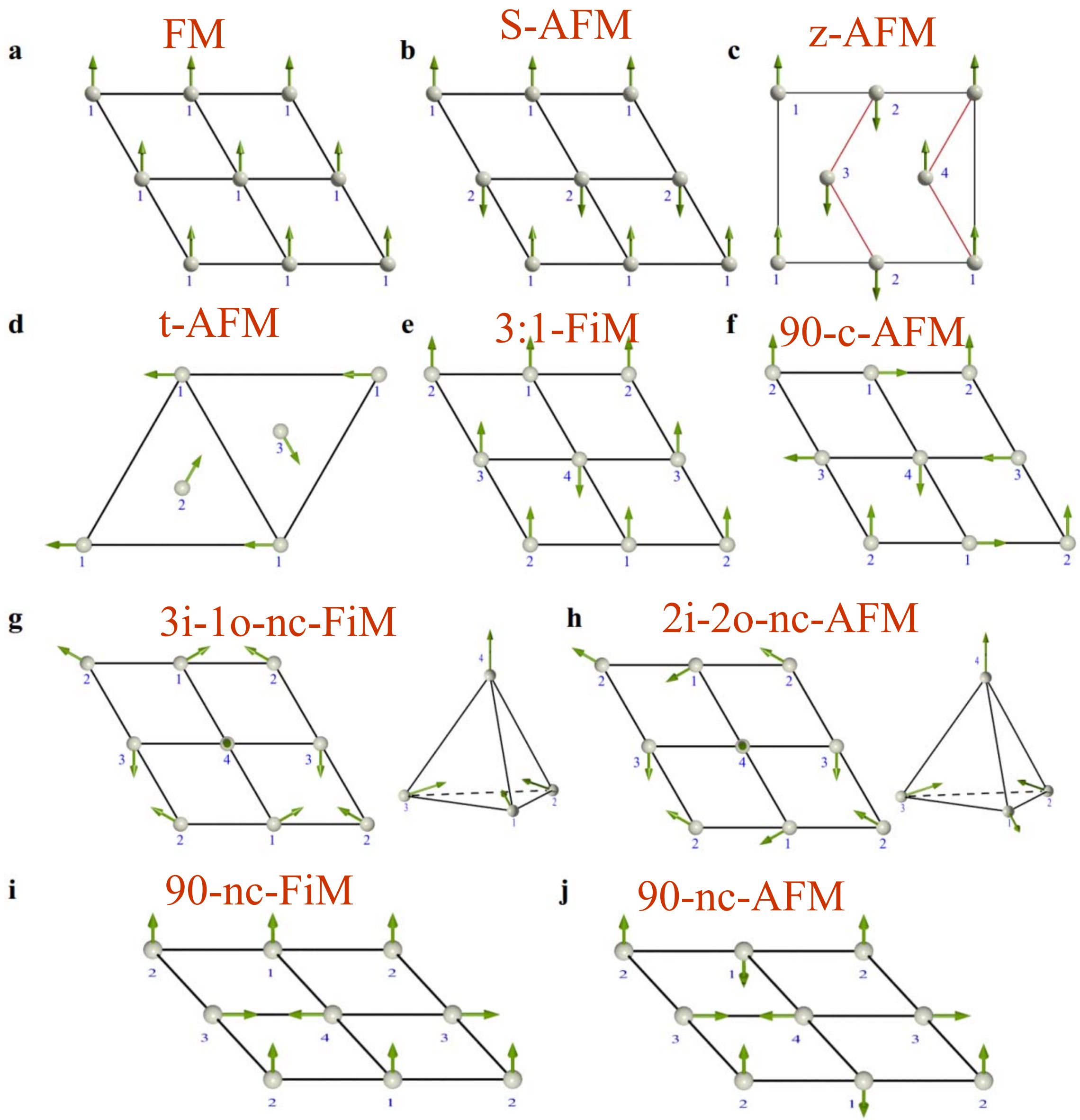

Ground state: all-in (all-out) non-coplanar antiferromagnetic structure.

Possible metastable magnetic structures

Total energy (ΔE^{tot}) (meV/f.u.), total spin moment (m_s^{tot}) (μ_B/f.u.), Rh atomic spin moment (m_s^{Rh}) (μ_B/f.u.) and band gap (E_g), from GGA+U calculations. [VASP-PAW method, GGA+U_{eff} (Rh) = 2 eV]

[Zhou et al., PRL 116, 256601 (2016)]

	ΔE^{tot}	m_s^{tot}	m_s^{Rh}	E_g
NM	20.19	0.00	0.00	metal
FM	2.48	0.50	0.36	metal
s-AFM	5.61	0.00	0.23	metal
z-AFM	12.85	0.00	0.23	metal
t-AFM	20.17	0.00	0.10	metal
3:1-FiM	1.99	0.00	0.06/0.15/0.24/-0.47	metal
90-c-AFM	2.20	0.00	0.23	metal
90-nc-AFM	2.14	0.00	0.23	metal
nc-AFM	0.00	0.00	0.24	0.22

Heisenberg model

$$H = E_0 - \sum_{i<j} J_{ij}\sigma_i \cdot \sigma_j$$

Exchange coupling

J_1 = 4.4, J_2 = -3.6 meV

Neel temperature T_N = ~20 K

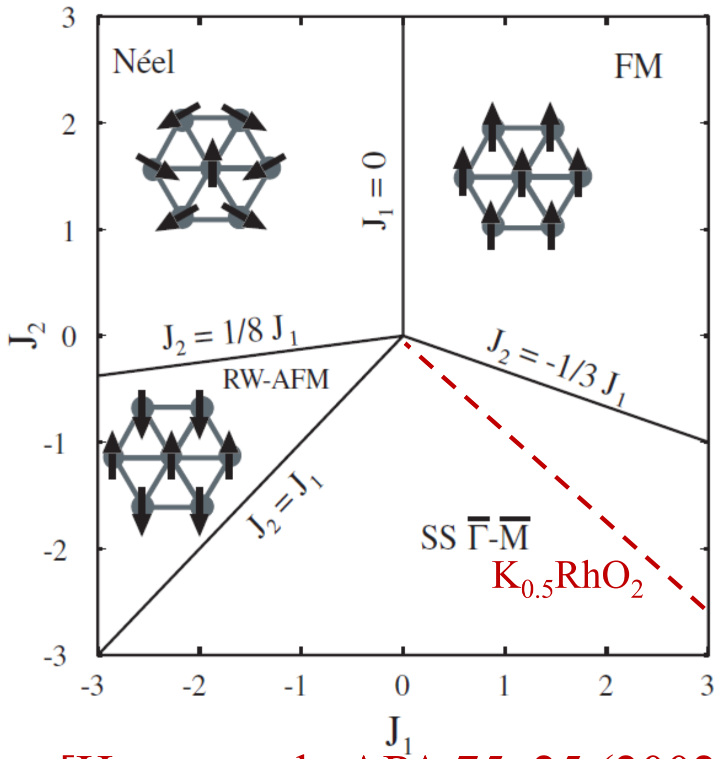

[Henze et al., APA 75, 25 (2002)]

2) Band structure of non-coplanar antiferromagnetic structure

[Zhou et al., PRL 116, 256601 (2016)]

An insulator (E_g =0.22eV) $8(K_{1/2}RhO_2)$

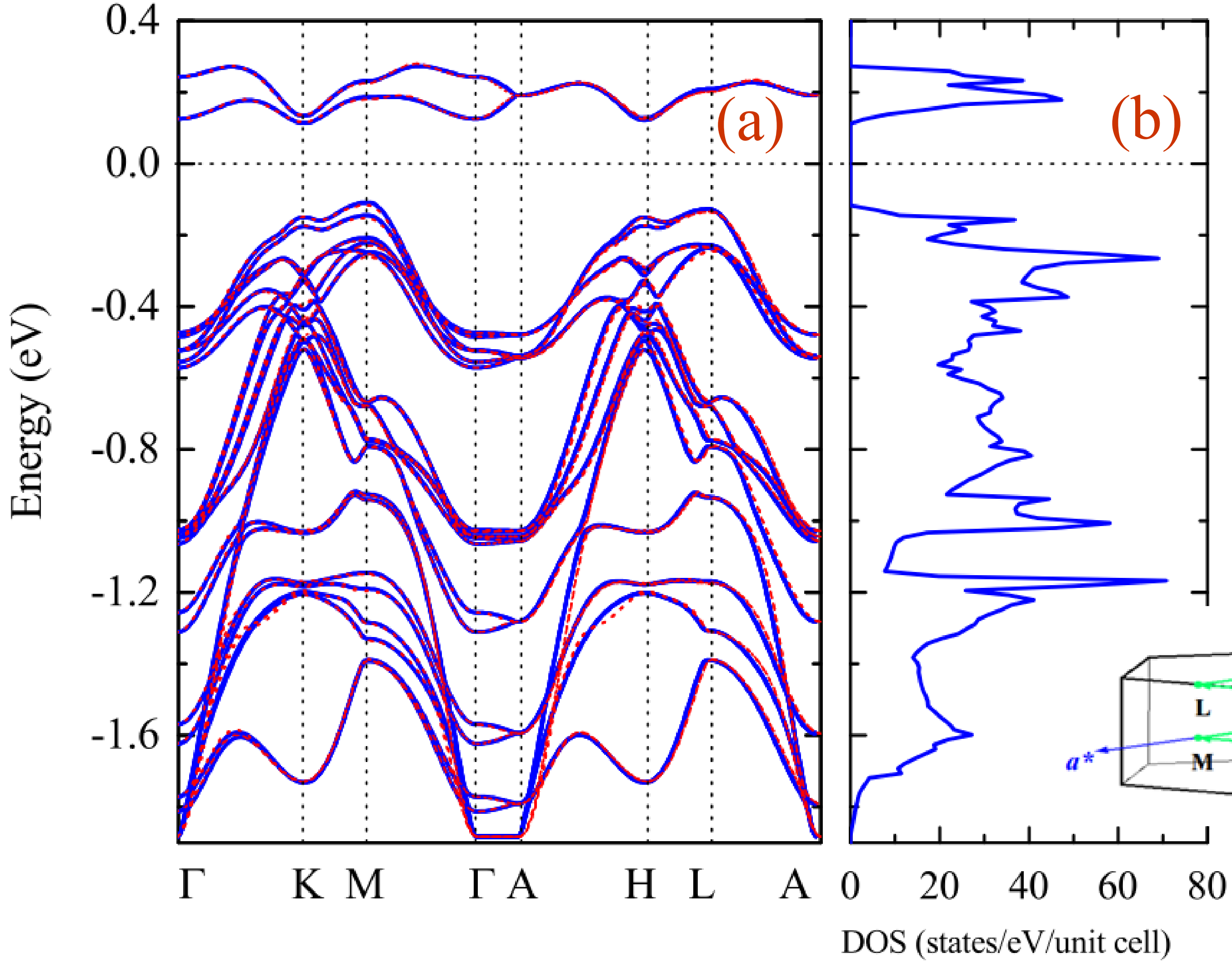

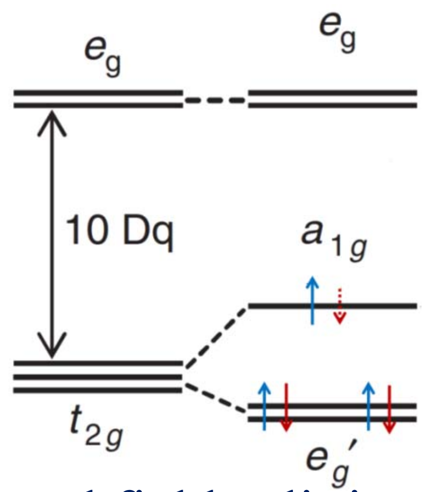

Crystal field splitting of Rh t_{2g} orbitals in $K_{1/2}RhO_2$ with Rh a_{1g} is ¾ filled.

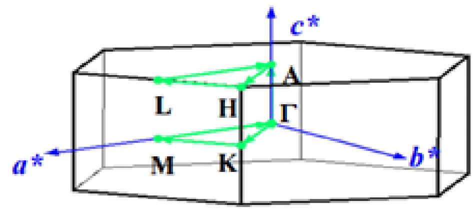

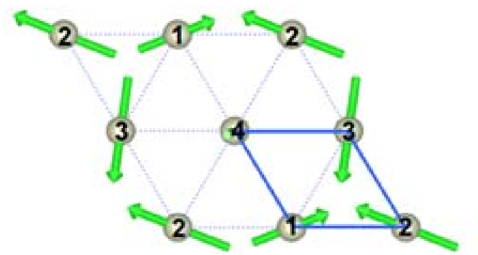

In (a), blue solid lines from GGA+U and red dotted lines from MLWFs interpolations.

Is it a topologically trivial or nontrivial insulator?

3. Unconventional quantum anomalous Hall phase

1) A Chern insulator

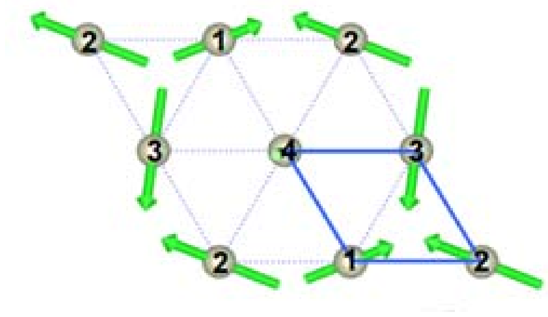

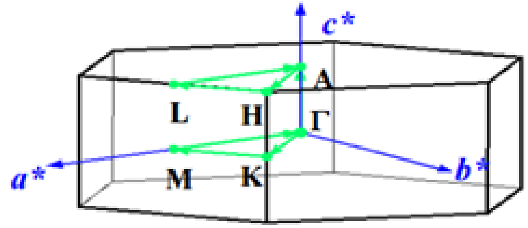

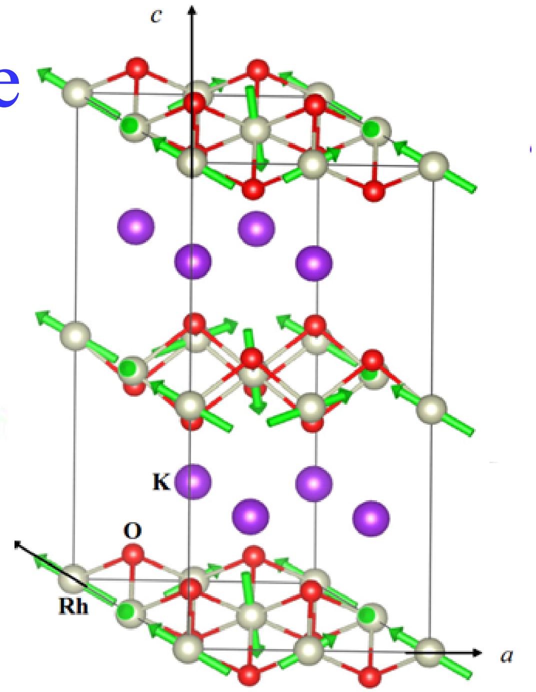

Anomalous Hall conductivity

$$\sigma_{AH} = -\frac{e^2}{\hbar(2\pi)^3}\int d^3k \sum_n f(\varepsilon_n(\mathbf{k}))\Omega_n^z(\mathbf{k})$$

$$\Omega_n^z(\mathbf{k}) = -\sum_{n'\neq n}\frac{2\,\mathrm{Im}\langle \mathbf{k}n|v_x|\mathbf{k}n'\rangle\langle \mathbf{k}n'|v_y|\mathbf{k}n\rangle}{(\omega_{\mathbf{k}n}-\omega_{\mathbf{k}n'})^2}$$

For a 3D Chern insulator,

$$\sigma_{AH} = n_c\frac{e^2}{hc}$$

n_c is an integer (Chern number)

Thus, nc-AFM state is a QAH phase with $n_c = 2$.

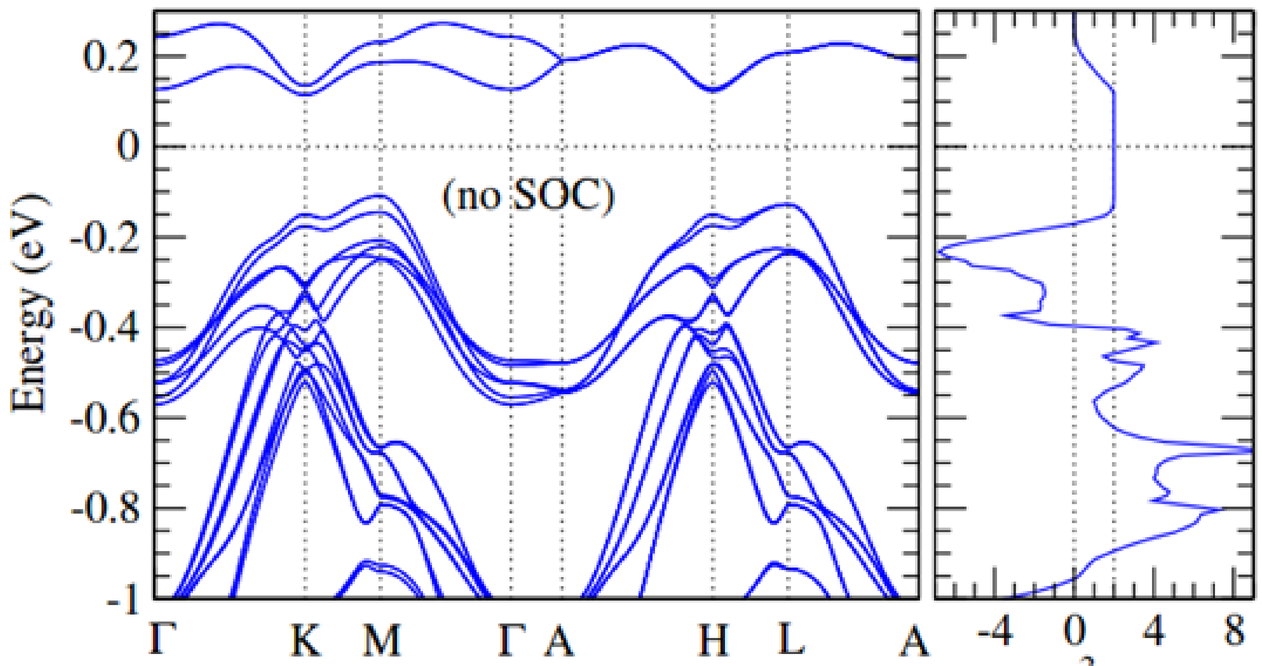

[Zhou et al., PRL 116, 256601 (2016)]

2) Edge states

[Zhou et al., PRL 116, 256601 (2016)]

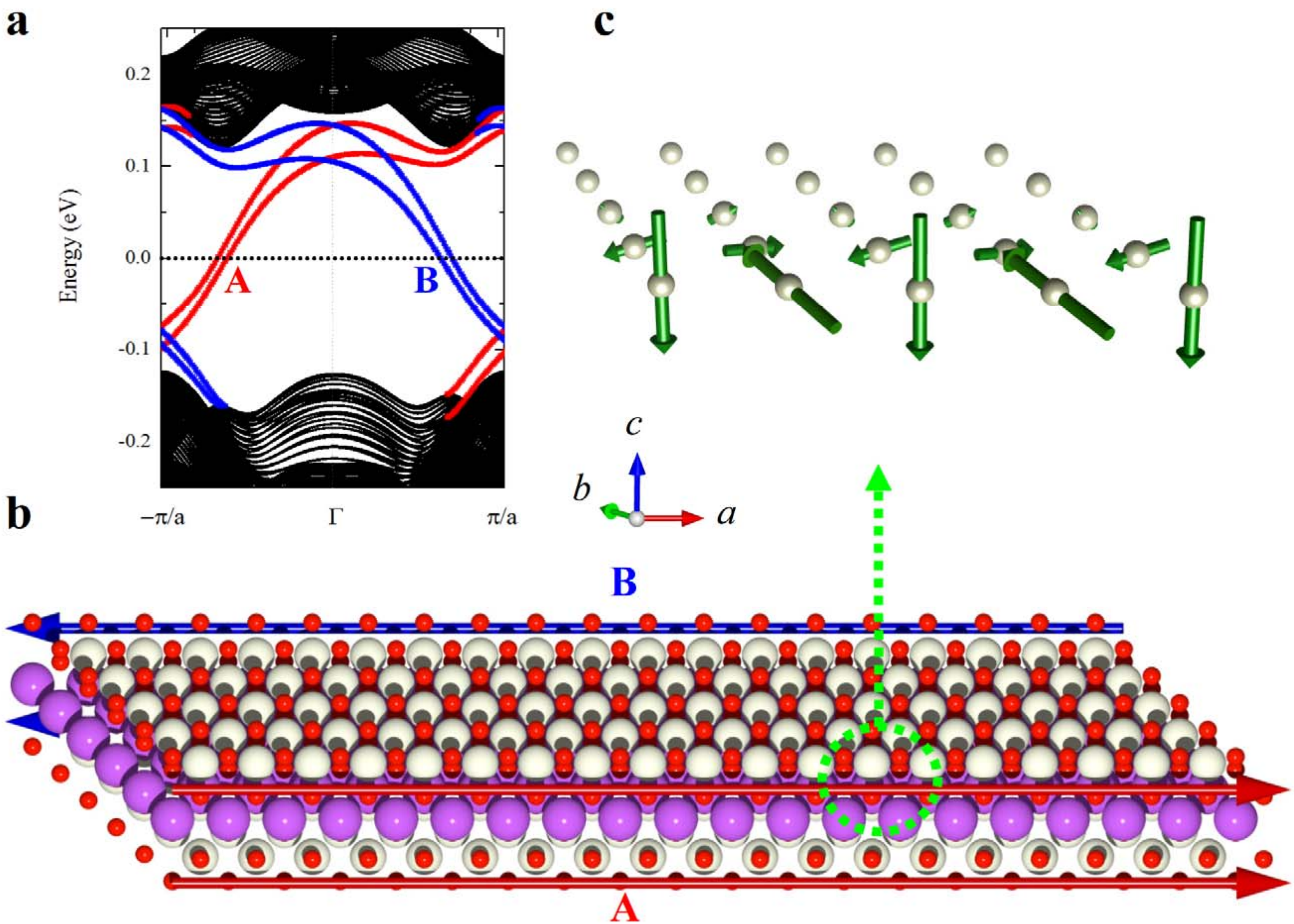

Bulk-edge correspondence theorem is fulfilled.

3) Nature of the quantum anomalous Hall phase

Spin chirality, Berry phase and topological Hall effect

[Taguchi et al., Science 291, 2573 (2001)]

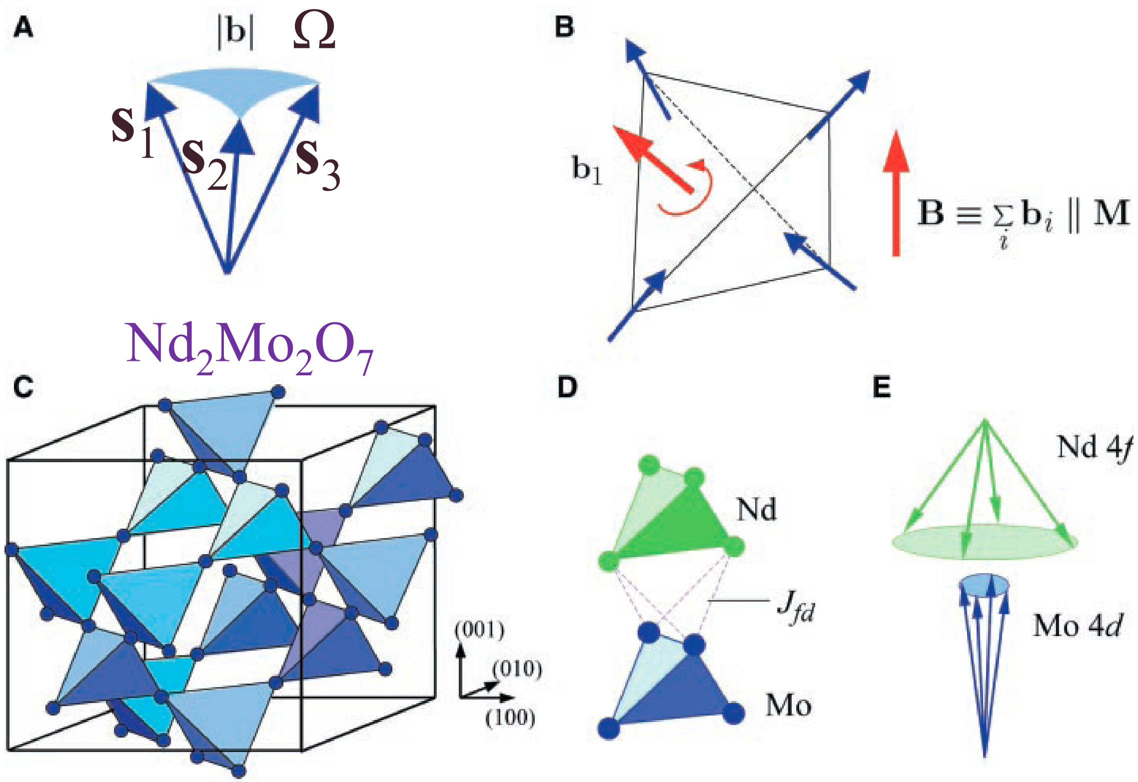

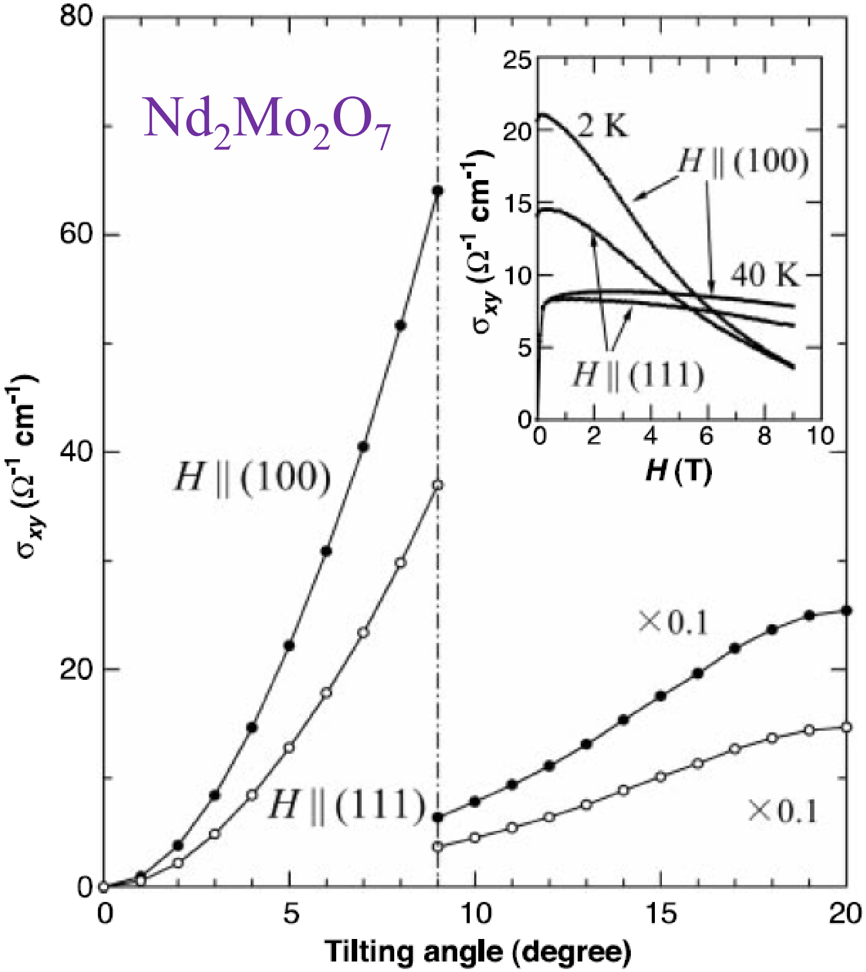

Spin chirality

$$\kappa = \sum_{i,j,k} \mathbf{s}_i \cdot (\mathbf{s}_j \times \mathbf{s}_k).$$

solid angle Ω,

Berry phase $\gamma = \Omega / 2$

Topological Hall effect: Anomalous Hall effect purely due to Berry phase produced by spin-chiraty in the noncoplanar magnetic strucure.

[Zhou et al., PRL 116, 256601 (2016)]

A conventional QAH phase is caused by the presence of FM and SOC!

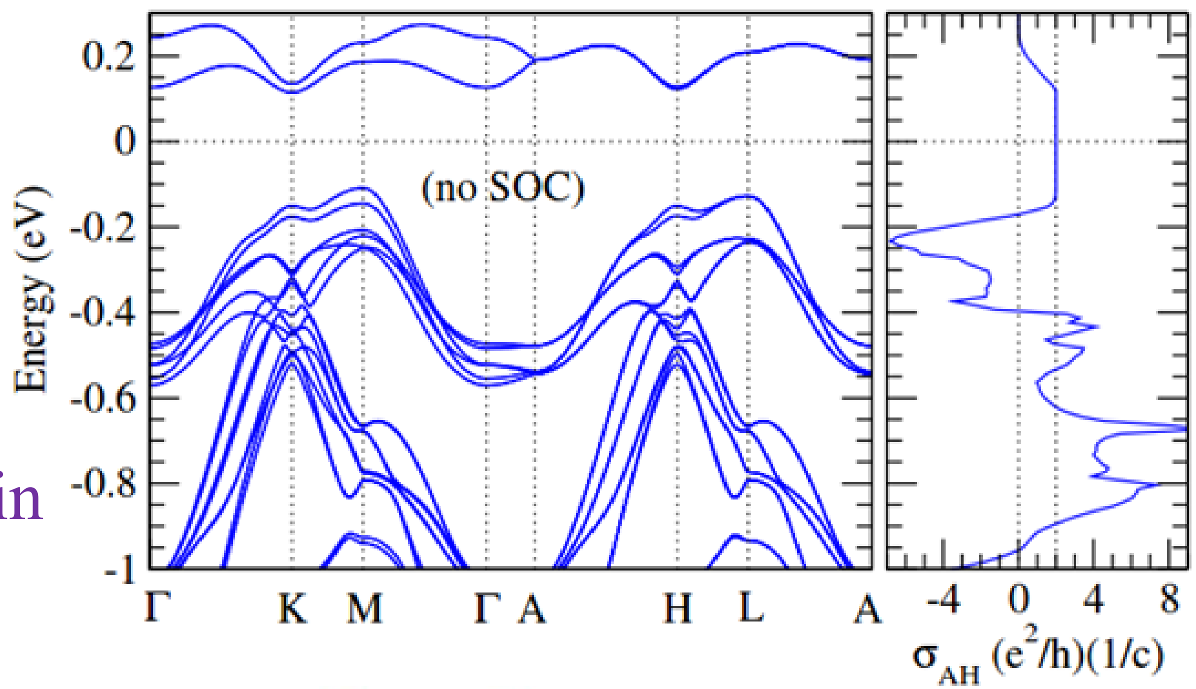

Here, $m_s^{tot} = 0$ and no SOC; thus QAH phase is unconventional.

AHC is due to nonzero scalar spin chirality in nc-AFM structure,

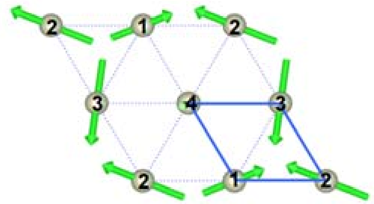

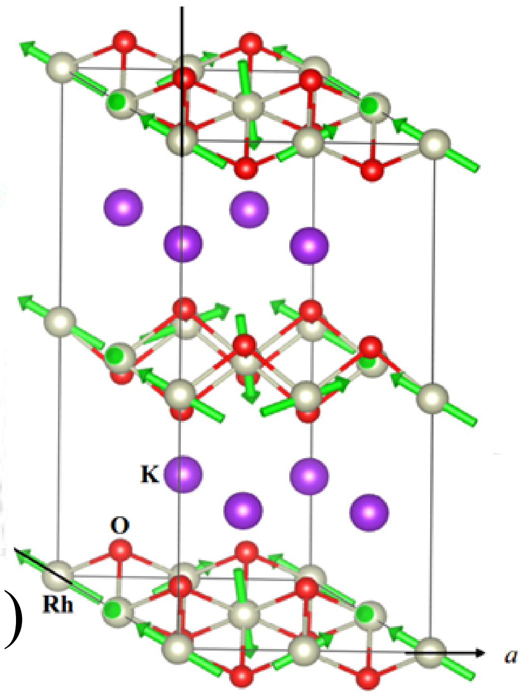

Total solid angle $\Omega = 4\pi$,

Berry phase $\gamma = \Omega / 2$,

Chern number $n_c = (\gamma / 2\pi) \times 2 = 2$,

AHC $\sigma_{AH} = 2e^2/h$.

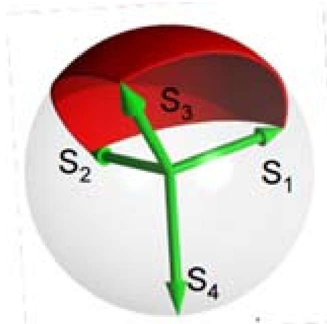

So it is the quantum topological Hall effect due to the topologically nontrivial chiral magnetic structure!

$$\kappa = \sum_{i,j,k} \mathbf{s}_i \cdot (\mathbf{s}_j \times \mathbf{s}_k)$$

4) Effects of spin-orbit coupling

[Zhou et al., PRL 116, 256601 (2016)]

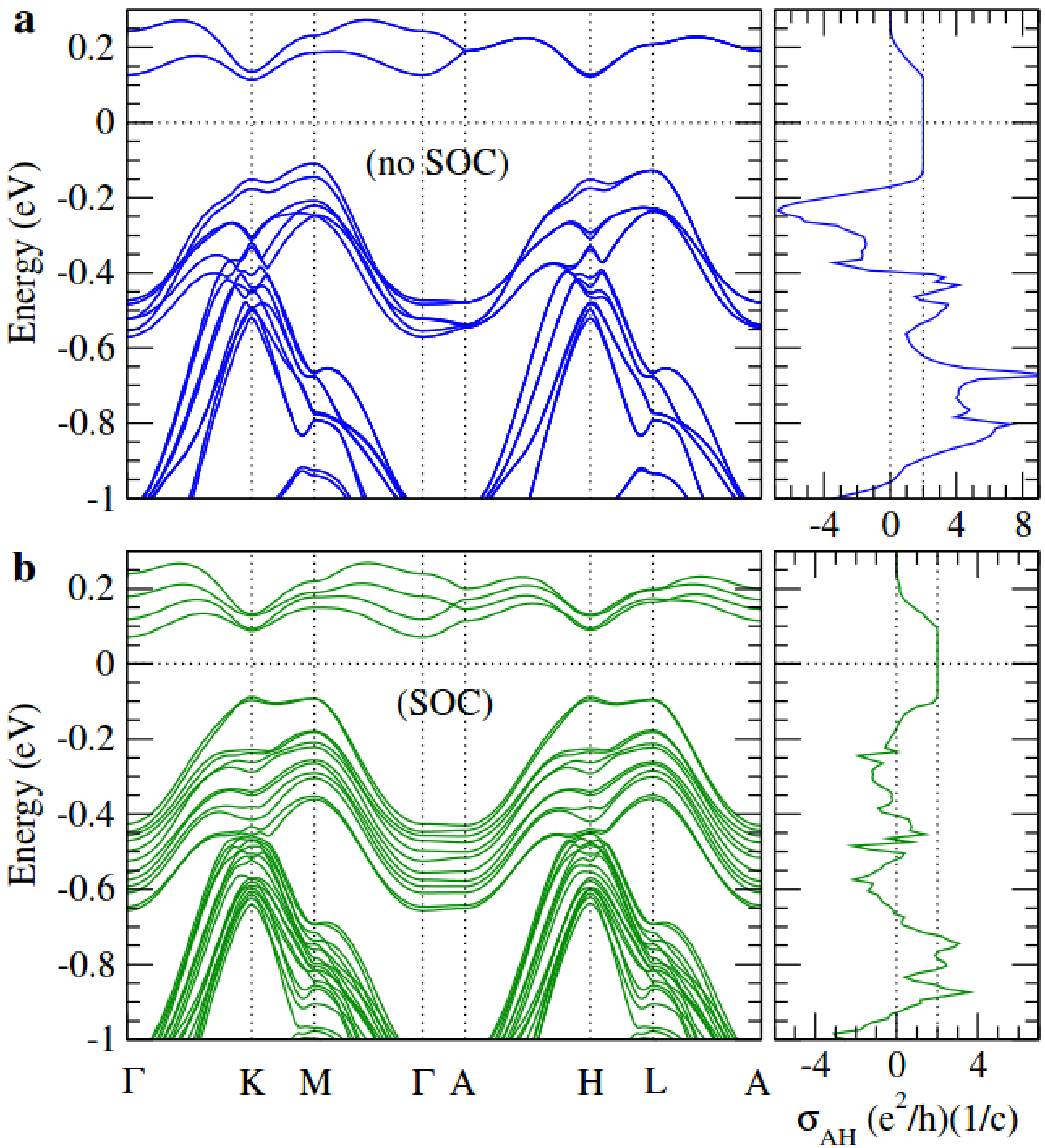

	ΔE^{tot}	m_s^{tot}	m_s^{Rh}	E_g
FM	2.61	0.46	0.33	metal
s-AFM	6.87	0.00	0.22	metal
z-AFM	13.59	0.00	0.21	metal
t-AFM	21.11	0.00	0.10	metal
3:1-FiM	3.55	0.01	0.21	metal
90-c-AFM	2.99	0.00	0.23	0.02
90-nc-AFM	1.90	0.00	0.19/0.22	0.05
nc-AFM	0.00	0.08	0.19/0.24	0.16

The nc-AFM structure remains the lowest energy one and it is still a QAH insulator with $E_g = 0.16$ eV and $m_s^{tot} = 0.08\ \mu_B$/f.u.

IV. Conclusions

1. Layered 4d and 5d transition metal oxides are good candidates for Chern insulators, because 4d and 5d transition metal oxides have stronger SOC but moderate/weak correlation, quite unlike 3d transition metal oxides where correlation is strong and often leads to Mott insulators.

2. Based on first-principles density functional calculations, we predict that the high temperature QAH phases would exist in two kinds of 4d and 5d transition metal oxides, ferromagnetic $/(LaOsO_3)_2/(LAO)_{10}$ perovskite [111] superlattice and layered chiral antiferromagnetic $K_{1/2}RhO_2$.

3. Further theoretical analysis reveals that the QAH phases in these oxide systems result from two distinctly different mechanisms, namely, conventional one of the presence of ferromagnetism and SOC, and unconventional one due to the topologically nontrivial magnetic structure (i.e., exotic quantum topological Hall effect).

Acknowledgements:

Discussion and Collaborations:

Hirak Kumar Chandra (Nat’l Taiwan U.)
Jian Zhou and his team (Nanjing U.)
Qi-Feng Liang (Shaoxing U.)

Supports:

Ministry of Science and Technology,
Academia Sinica (Thematic Research Program),
National Center for Theoretical Sciences of Taiwan.